CHARACTERIZING UPTAKE, DISTRIBUTION AND FATE OF CdSe/ZnS QUANTUM DOTS IN *SYNNECHOCOCCUS ELONGATUS* PCC7942

BY
SUN MIN KIM

THESIS

Submitted in partial fulfillment of the requirements
for the degree of Master of Science in Agricultural and Biological Engineering
in the Graduate College of the
University of Illinois at Urbana-Champaign, 2011

Urbana, Illinois

Advisers:

Assistant Professor Kaustubh Bhalerao
Professor Rashid Bashir

ABSTRACT

One of the challenges in developing a framework for characterizing nanoparticle toxicity is that the number of nanoparticles and their superficial derivatives is very large and continues to expand rapidly. Multiple factors such as size, geometry, surface chemistry, nanoscale topology, electromagnetic activity, and aggregation and degradation processes can modify the original nanoparticle and change its behavior significantly. Secondly, the type of environments and organisms these nanoparticles may be subjected to are also numerous and complex. Thirdly, the number of analytical and computational techniques available to the researcher today spans physical, chemical, biomolecular, ecological and '-omics' based approaches. Thus any combination of nanoparticle, model organismal system and analytical technique is a potential route of investigation and can produce important broad empirical information on the impact of nanomaterials on living systems.

This study is an extension of the analytical framework called DIMER, which involves characterizing the dispersion, imbibition, metabolism, elimination and recycle of nanoparticles to study its life cycle of in the environment. Cadmium selenide quantum dots coated with zinc sulfide were chosen as a model nanoparticle. Similarly the cyanobacterium *Synechococcus elongatus* PCC 7942 were chosen as the model host organism.

This study characterizes the uptake, distribution and fate of both water insoluble and water soluble CdSe/ZnS quantum dots in cyanobacteria. To quantify the toxicological impact of quantum dots on cells, cell growth rate, membrane destabilization, viability and the activity of photosynthetic pigments were characterized. For characterization of uptake and distribution, flow cytometry, laser scanning confocal microscopy and transmission electron microscopy were used. When quantum dots are dispersed into the environment, their imbibition, metabolism, degradation and elimination from cells depends on their surface coating. Consequently, water soluble quantum dots, which are coated with a hydrophilic coating, showed dramatically reduced degradation rates and resulting hazardous effects on the cells even when observed directly in contact with the cells. However, water insoluble quantum dots were immediately toxic to the cells. The observed toxicity was largely indistinguishable from cadmium toxicity, which is a degradation product of the quantum dot. The primary impact observed is that the cadmium destroys the photosynthetic machinery of

the cells. Given the central role of cyanobacteria in many aquatic ecosystems, such damage has serious implications to an ecosystem. Additionally, the cadmium toxicity is persistent in the environment. Once contaminated, the growth media continues to inhibit the growth of new cyanobacteria indicating a long-lasting, toxic effect on the environment.

ACKNOWLEDGEMENTS

My graduate study would not have been finished without many people. First and foremost, I would like to express my gratitude to Dr. Kaustubh Bhalerao for his guidance, support and patience to successfully complete all my graduate studies at UIUC. He always encouraged me to have many questions, which helped me to develop critical thinking and instilled confidence in me. I would also like to express my sincere thanks to co-advisor, Dr. Rashid Bashir for introducing me various nanotechnology applications. I deeply thank my committee, Dr. Prasanta Kalita for his valuable insight and guidance towards completing the thesis.

I thank Phil, Vaisak, Rekha and Goutam to have great time together in the lab. I have lots of great memories in Champaign with Jinhae, Yoon Ju, Patricia, Hyun Seung, Jong Min and SangHoon. Thanks go also to my friends in the Department of Agricultural and Biological Engineering.

I also want to thank all my friends and family in Korea. My parents, Si Ju Kim and Jung Hee Kim have always provided encouragement and support.

TABLE OF CONTENTS

Chapter 1. INTRODUCTION

1.1. DIMER: Need for a framework for understanding the environmental impact of nanotechnology

Applications of engineered nanoparticles are becoming increasingly commonplace. Nanomaterials offer superior mechanical, electromagnetic and chemical properties, some of which are a result of particle sizes in the 1-100 nm size scale. There are various examples of engineered nanoparticles used in daily products such as cosmetics (Xia et al., 2010; Wokovich et al., 2009), soap, and food packaging (Monteiro et al., 2009; Zhang et al., 2010). Engineered nanoparticles are also used in imaging-based diagnostic and drug delivery (Xing and Rao, 2008; Michalet et al., 2005; Xing et al., 2009), monitoring of tumors (Jaiswal and Simon, 2007; Su et al., 2010) and therapeutics (Xing and Rao, 2008; Ho and Leong, 2010; Yang, 2010). Given their novel and impactful applications, the possibility that nanoparticles are being dispersed into the environment by accidental and intentional means is also clearly on the rise. Since nanoparticles can possess different chemical and physical properties when compared with constituent bulk materials, a new approach for risk assessment that takes into account the nanoscale nature of these materials is needed.

A framework abbreviated 'DIMER' was proposed to elucidate potential impact of nanoparticles on the environment and to generate comprehensive risk profile of them (Figure 1-1). DIMER stands for Dispersion, Imbibition, Metabolism, Elimination and Recycle. It is adapted from the pharmacological framework of ADME/Tox (absorption, distribution, metabolism, excretion, toxicology). The main difference between the two frameworks is that nanoparticles in the environment exhibit bioaccumulation and recycle via different environmental media or the food chain, which does not have a direct analogue in the existing pharmacological framework. Current methodologies of understanding nanoparticle toxicity are focused on a subset of the DIMER framework (Mahendra et al., 2008; Hardman, 2006; Magrez et al., 2006).

Once nanoparticles are dispersed into the environment, they travel through different environmental media (air / water / soil), are taken up by organisms or demonstrate altered particle properties due to oxidation, aggregation etc. In some cases, these released

nanoparticles can be sequestered and removed from circulation, while in other cases, they could redisperse into the environment in an intact or altered form. Thus, all phases of the life cycle of nanoparticles should be considered in order to develop a comprehensive risk profile (Oberdörster et al., 2005). While the DIMER framework provides a graph of the potential paths taken by the nanoparticle through the environment, a suite of analytical tools are required to fill in our gaps in knowledge in order to provide predictive analysis on the potential paths a nanoparticle might take through the environment and the biosphere. This analytical cascade should span the entire range from physical and chemical tests to ecological perturbation analysis as depicted in Figure 1-2. The more mechanistic the characterization, the better we might be able to predict properties of stability / mobility / toxicity for various families of nanoparticles. The DIMER framework helps organize the multi-faceted information on nanoparticle toxicity and its impact on the environment. It can therefore serve as a resource for developing policy and educational guidelines, as well as material handling and processing protocols for nanomaterials.

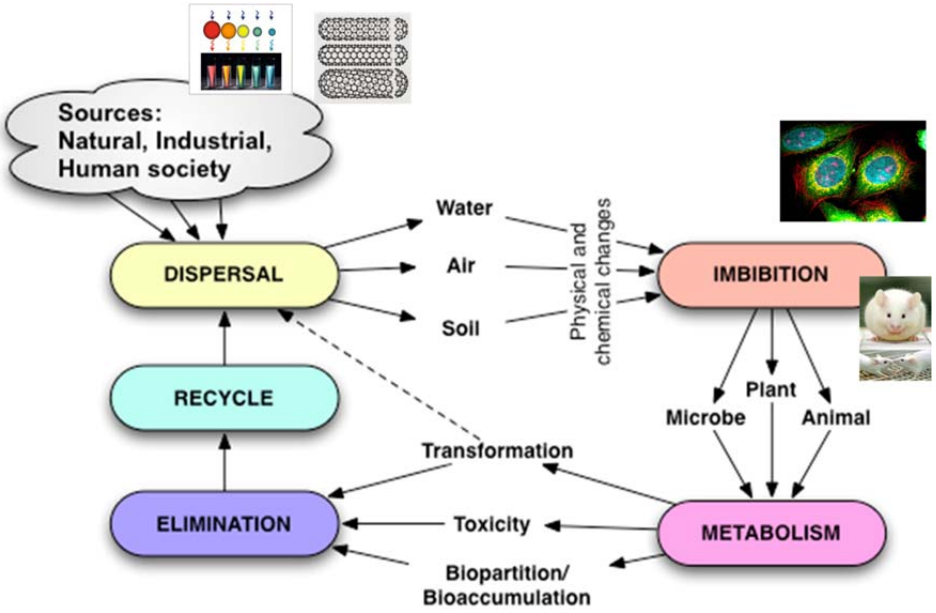

Figure 1-1. The DIMER framework. The life cycle of a nanoparticle through the environment and its interaction with the biospehere is modeled in this graph.

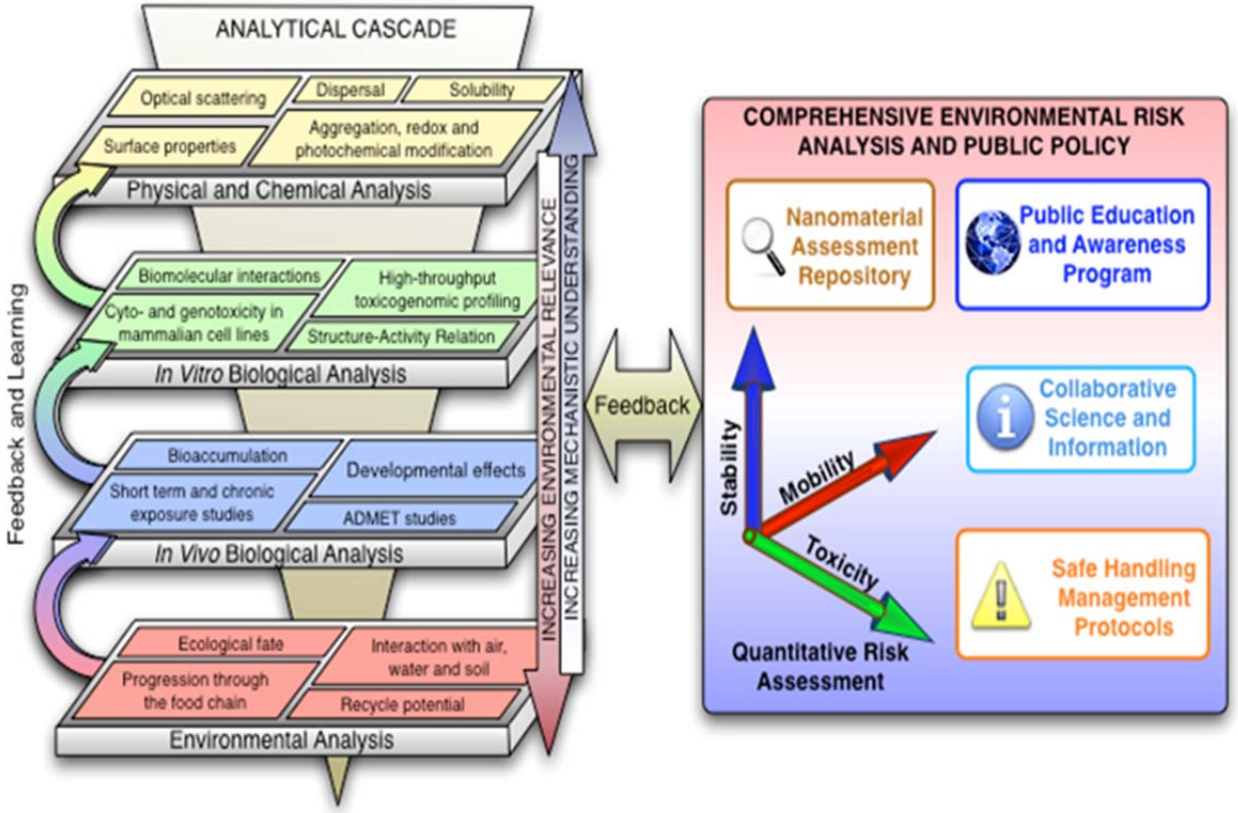

Figure 1-2. Analytical cascade for developing DIMER concept. 1Various levels of analysis from the physical / chemical to the environmental help provide information on the various aspects (stability, mobility and toxicity) of a nanoparticle, which in turn provides the basis for sound policy and safety recommendations.

Dispersion, Elimination and Recycle

First and foremost aspect of environmental release of any engineered nanoparticle is its mode of dispersion. Nanoparticles could be released in the process of manufacture, usage, and disposal. Mueller and Nowack (2008) estimated that 500 t/a of nano silver, 350 t/a of carbon nanotubes and 5000 t/a of nano titanium dioxide were produced worldwide in 2007/2008. During the manufacturing process, they could be dispersed as aerosols or manufacturing wastes. Blaser et al. (2008) proposed dispersion mechanisms for nano-silver, which is known to have antimicrobial activity and is used as a component of biocidal plastics and textiles. Silver nanoparticles would be dispersed into environment while the plastics and textiles discharge through untreated wastewater, treated wastewater and solid waste.

Another common example of nanoparticle dispersion is that of nanoparticulate titania. Nano-TiO_2, with its high reflectivity and ability to scatter ultraviolet, is used in cosmetics, especially sunscreen. Once the sunscreen is washed off, the majority of the nanoparticles end up in the sewage. Thus nanoparticles, when used in high volumes, can potentially travel through the aquatic, terrestrial or atmospheric routes. Moreover, nanoparticles could move through food chain by accumulating in the organismal tissues. If nanoparticles have long residence times in cells, they could affect higher level of organisms in the food web.

Imbibition

Once nanoparticles are exposed to the environment, they can enter into the ecosystem via several uptake routes depending upon the organism. Inhalation, transdermal absorption and ingestion are the main pathways that nanoparticles enter into higher organisms. Inhaled nanoparticles attack the respiratory tract and can translocate to other organs. Aquatic organisms can take up nanoparticles via the gill epithelium or the digestive tract. Zhang et al. (2006) showed that TiO_2 nanoparticles are accumulated in the viscera and gills of carp. 10 nm gold nanoparticles adsorbed on the cell wall of algae. As the algae are consumed by clams, the nanoparticles penetrated clam's gills and accumulated in the digestive epithelia and damaged intracellular organelles (Renault et al., 2008). Similar studies on nickel nanoparticles showed that they were localized within the digestive system lumen in zebrafish embryo (Ispas et al., 2009).

It is generally difficult to determine whether low level organisms in the ecosystem are more sensitive than higher level organisms or vice versa. Even when different types of bacterial cultures are exposed to the same nanoparticle, the cultures showed differential toxicities, indicating that the overall risk is a result of a combination of a variety of elements and the environment. Comparing the gram positive *B. subtilis* and the gram negative *E. coli*, *E. coli* is more resistant to the CdTe quantum dots but is more susceptible to SiO_2, TiO_2 and ZnO (Dumas et al., 2009; Adams et al., 2006). On the other hand, different allotropes of carbon are differentially toxic to a single organism. Carbon nanotubes exhibited more hazardous effects than carbon black to mice (Lam et al., 2004). Similarly, Navarro et al. (2008) observed that silver nanoparticles showed higher growth inhibition than same silver concentration of $AgNO_3$ on green algae, *C. reinhardtii*.

At the cellular level, nanoparticles cross the cell membrane via endocytosis. In this process, the membrane extends and engulfs the particles, which cannot directly cross the plasma membrane, to enter into the cells. The endocytosis may occur through lipid rafts as well as cell membranes. This method of uptake is categorized as phagocytosis or pinocytosis. The latter can be further sub-divided into macropinocytosis, clathrin-mediated endocytosis and caveolae-mediated endocytosis. Phagocytosis engulfs solid particles, whereas pinocytosis makes vesicles of fluid. Macropinocytosis is a non-specific form of endocytosis and involves relatively large fluid vesicles (>1µm). Clathrin-mediated and caveolae-mediated endocytosis are specific receptor-mediated forms of endocytosis. Clathrin-mediated endocytosis which exists in all kinds of cell types has receptors in clathrin-coated pits on plasma membrane and forms engulfing vesicles size less than 120 nm. Caveolae-mediated endocytosis involves flask-shaped invaginations in the plasma membrane and forms less than 60 nm size of vesicles (Conner and Schmid, 2003). Endocytosis is a size- and surface charge-dependent process. Positively charged nanoparticles are more likely to vigorously bind to the negatively charged cell surface moieties, and are therefore more likely to translocate across the plasma membrane (Verma and Stellacci, 2010). ZnO anoparticles were internalized by endocytosis and localization in vesicles of *Euglena gracilis* (Brayner et al., 2010). Zhang and Monteiro-Riviere (2009) observed that the carboxylic acid group of quantum dots were first recognized by the lipid rafts. In contrast, cells absorb TiO_2

nanoparticles by engulfing them via endosomes and localizing them in the lysosomes. In some cases, they may also accumulate in the mitochondria (Braydich-Stolle et al., 2009).

Metabolism

Cells undergo various toxic effects after uptake nanoparticles. A review paper of Nel et al. (2006) describes the numerous perturbations on cells exposed to nanoparticles. These include the generation of reactive oxygen species (ROS) and consequent oxidative stress, mitochondrial perturbation (eg: energy failure, membrane damage…), inflammation, altered cell cycle regulation, DNA damage and more.

1.2 Case for using quantum dots (QDs)

Quantum dots are artificial atoms with a core-shell structure. The core part consists of cadmium, which is the frame element, along with another chemical, either selenium, sulfur or tellurium. The CdSe (or CdTe / Cd/S) core is responsible for unique fluorescent properties. By constraining the CdSe in a very small space, the quantum dot is often represented as a material with zero dimensions. The constrained size has the effect of limiting the energies that the electrons of CdSe composite may have. This leads to the observed fluorescence properties. The fluorescent core is protected by an encasing shell, which is usually composed of a zinc sulfide. The ZnS shell is frequently modified with various functional coatings to achieve suitable surface properties of solubility or surface interaction. In addition to modifying surface properties, functional groups protect quantum dots from U/V light and limit degradation. The fluorescence emission wavelength can be tuned by adjusting the size of the quantum dot core. With their high photostability, quantum yields and tunable emission characteristics, quantum dots find broad applications in monitoring and diagnostics. Well-established areas of application include tumor imaging (Gao et al., 2005; Bagalkot et al., 2007), as well as imaging intracellular properties and structure (Derfus et al., 2004a; Sukhanova et al., 2004).

Their degradation of quantum dots and the release of their components under light and high temperatures are well understood. There are several studies investigating the temporal decay in the efficiency of optical properties using higher organisms (King-Heiden

et al., 2009) and mammalian cells (Derfus et al., 2004b) as model cultures. For evaluating toxicity, the released heavy metal components play a significant role following quantum dot degradation. This toxicity might show synergistic effects combining heavy metal and quantum dots, or toxic effects unique to nanomaterials. King-Heiden et al. (2009) studied quantum dots toxicity using zebrafish embryos, and found that their toxicity is similar to cadmium toxicity, along with some toxicity that was unique to quantum dots. Toxicity evaluation of quantum dots is generally more complex because of degradation. However, since there is much information about heavy metal toxicity, separate toxicity studies on nanomaterials serve to illuminate the differential aspects of nanomaterial toxicity when compared with heavy metal toxicity.

Although many biological applications of quantum dots, such as imaging and drug delivery using quantum dots, have been studied, their application has been extended to include quantum computers and opto-electronic devices (Coe et al., 2002; Press et al., 2008). As more quantum dots applications appear on the market, and the probability of environmental release correspondingly increases. It is therefore necessary to generate a comprehensive risk profile of quantum dots and their ultimate fate in the environment, to the degree it can be estimated.

1.3 Case for using cyanobacteria

Cyanobacteria are prokaryotic, photosynthetic unicellular organisms living in aqueous environments. They are also known as blue-green algae. Cyanobacteria have played a key role in the evolution of life on the planet, as they are regarded as a pioneer for oxygenic photosynthesis and oxygen respiration (Herrero and Flores, 2008). In addition to generating an oxygen-rich environment 3500 million years ago, cyanobacteria are also considered to be the precursors of green plants. Although the details of the evolution of an eukaryotic organism are still being debated, endosymbiosis is a generally accepted mechanism in eukaryotic evolution. Plant organelles such as chloroplasts are thought to have originated as endosymbiotic cyanobacteria (Archibald, 2009; Okamoto and Inouye, 2005).

Along with evolutionary significance, cyanobacteria are also highly adaptable. It is easy to find cyanobacteria regardless of environmental conditions. They live in extremely hot and cold temperatures, salty conditions, and within a wide range of pH. Their high tolerance for extremely harsh conditions might help their evolvability and provide a better understanding of mechanisms for coping with environmental stresses (Hagemann, 2011; Marin et al., 2006; Ozturk and Aslim, 2010; Pandhal et al., 2009; Tamoi et al., 2007).

Being primary photosynthetic producers, cyanobacteria form the foundation of an aqueous ecosystem. They are at the bottom level of the food chain and can significantly impact a given ecosystem. Cyanobacterial blooms can cover the surface of an aqueous system and affect the quality of water, by preventing light to enter, depleting oxygen or the producing odor. Some species can also produce toxic substances harmful to other aqueous living things, which could induce die–offs of entire organisms, causing system-wide disruption of ecosystems (Saker et al., 2009).

Given their relevance to aqueous ecosystems and the sensitive dependence of ecosystems on cyanobacteria, the following six points summarize the merits of choosing cyanobacteria as a model for evaluating the environmental impact of nanoparticles:

1) They are prolific and form the food source for a number of aquatic species, which has profound implications, due to bioaccumulation and biomagnification.

2) They are relatively easy to cultivate in a laboratory.

3) Tools for molecular genetics and bioinformatics exist, which can allow for analysis using systems biology tools.

4) They are a potential candidate for deploying mitigation strategies for cleanup in aquatic environments.

5) They serve to elucidate the mechanism of ingress of environmental contaminants into an ecosystem in a realistic manner.

6) Their evolutionary relationship to cell organelles such as mitochondria and chloroplasts might provide predictive insight into the impact of quantum dots on cellular organelles of higher organisms.

1.4 Objectives of the present study

This study is mainly focused on understanding the toxicity of CdSe/ZnS nanoparticles on a species of freshwater cyanobacterium. The study is framed using the DIMER concept, which provides guidelines on interpreting the analytical results in the context of environmental release. We study ecosystem integrity using the simplest organism, cyanobacteria *Synnechococcus elongatus* PCC7942, as a result of an accidental dispersal of nanoparticles especially quantum dots. Objectives of this study are as follows:

1) Characterizing water insoluble quantum dots and water soluble quantum dots before dispersal into the model culture media. (Dispersion) Physical and chemical properties of particles would determine the uptake mechanism and interaction with cyanobacteria. As different types of nanoparticles would show different results, similar nanoparticle composition with different surface properties are expected to show unique toxic effects.

2) Characterizing the uptake mechanism and distribution of quantum dots in cells. (Imbibition) How nanoparticles enter into cells and how they are distributed among the various compartments will be studied. This will elucidate the relationship between the uptake and the fate of cells.

3) Characterizing the fate of cells exposed to quantum dots. (Imbibition / Metabolism) This task seeks to understand the relationship between biodistribution within cells and the resulting organism-wide impact measured via growth rate and photosynthetic ability.

4) Characterizing media contamination. (Elimination / Recycle) If inorganic nanoparticles produce a toxic response, lead to the death of the organism exposed to them, and are subsequently re-released into the environment, they can potentially accumulate and continue to elicit such toxic responses in new organisms.

Chapter 2. BACKGROUND AND LITERATURE REVIEW

2.1 Nanomaterial

Terminology and properties

The discipline of nanotechnology is built around the exploitation of materials, which show unique physical properties at nanometer size scales, that are not normally observable at larger scales. In 2005, International Organization for Standardization (ISO) established the ISO TC229 for standardization in the field of nanotechnologies. It defines nanotechnologies to include either or both of the following:

> *1) understanding and control of matter and processes at the nanoscale, typically, but not exclusively, below 100 nanometres in one or more dimensions where the onset of size-dependent phenomena usually enables novel applications,*
>
> *2) utilizing the properties of nanoscale materials that differ from the properties of individual atoms, molecules, and bulk matter, to create improved materials, devices, and systems that exploit these new properties.*

Nanomaterials are defined as materials with any external dimension in the nanoscale or having internal structure or surface structure in the nanoscale. They can be divided into nano-objects and nanostructured materials. Nano-objects are materials with one, two or three external dimensions in the nanoscale. Nano-objects in turn are classified as nanoplates, nanofibres, and nanoparticles by external dimension.

A quantum dot is defined by the European Standardization Committee and International Organization for Standardization (CEN ISO/TS 27687) as crystalline nanoparticle that exhibits size-dependent properties. As particle sizes decrease, physical phenomena resulting from weak forces such as van der Waal's forces and electrodynamic quantum effects become increasingly influential in the overall properties of the nanomaterials. Quantum confinement of the electronic states appears and the energy band gap becomes larger and discrete and resembles atoms. In the case of quantum dots composed of a core and shell architecture, they have three-dimension quantum confinement (total confinement) and display the property of fluorescence. Different

fluorescence emission of quantum dots can be obtained by adjusting the size of quantum dots. This property of fluorescence is not observed in the bulk materials.

Regulation for nonmaterial's

Nanotechnology and nanomaterials have productive applications in the areas of energy, cosmetics, healthcare and agriculture. Among many types of nanomaterials, single-wall and multi-wall carbon nanotubes were first regulated by the U.S. Environmental Protection Agency (EPA) under Significant New Use Rules (SNURs). Not only EPA, but also other regulation agencies such as U.S. Food and Drug Administration (FDA), Organization for Economic Co-operation and Development (OECD) and European Union (EU) are discussing regulatory schemes for nanotechnology. To produce predictive information on nanoparticle toxicity for the risk assessment and regulations, it is necessary to develop appropriate experimental platforms to analyze physicochemical and environmental properties of nanomaterials, which differ with bulk materials (Powers et al., 2006).

Properties of nanomaterials for risk evaluation

Size, shape, solubility, chemical composition and surface properties are important in determining the toxicity of nanoparticles. Moreover, different synthetic process of manufactured nanoparticles of same chemical composition showed different toxic effects Tri-n-octylphosphine oxide (TOPO) or polyoxyethylene stearyl ether (Brij-76) was used as protective agents to control particle size and shape of nanoparticles during the synthesis. ZnO nanoparticles with tri-n-octylphosphine oxide (TOPO) showed acute toxicity to *Anabena flos-aquae* than particles with polyoxyethylene stearyl ether (Brij-76) (Brayner et al., 2010). Also, properties of nanoparticles could be changed and particles may become toxic after dispersion to the environment. For example, quantum dots could release toxic heavy metal ions (such as Cd) upon exposure to U/V light or high temperature (Derfus et al., 2004a).

Size is one parameter of nanomaterials that determines the mechanism of entry, deposition, translocation, and elimination of nanoparticles within an organism. Chemical and biological reactivity with the cells is increased as size of particles decreases (Hildebrand et al., 2009; Nutt et al., 2006). Typically, particles size below 20 to 30 nm change the crystallography of the particle through the rearrangement of the surface atoms or crystal

lattice contraction to achieve a more stable energy state (Auffan et al., 2009). These modifications can enhance the toxicity of particles to organism and environment. Chithrani et al. (2006) demonstrated the influence of particles size on intracellular uptake rate. 50 nm of gold nanoparticle showed maximum uptake rate than other sizes since the size seems best suited for receptor-mediated endocytosis. Moreover, the original particle size seems to be as important as aggregate size in case of particles that aggregate. For instance, both 10 and 100 nm TiO2 particles aggregated to 1,800 nm aggregates, but the smaller particles were more toxic to the cell (Braydich-Stolle et al., 2009).

Surface properties including specific surface area, surface chemistry and surface charge have to be characterized for risk assessment of nanomaterials. Physical and chemical properties are governed by surface properties. For example, surface charge determines the dispersion stability in solution and absorption rate at cells' surface. Surface coating and covalent surface modifications are exploited to improve biocompatibility. For example, quantum dots without a functional coating are more vulnerable to U/V and oxidative degradation. They are prone to degrade into their elemental constituents, chiefly Cd and Zn The leached heavy metal from core is toxic to organisms (King-Heiden et al., 2009; Derfus et al., 2004b; Hauck et al., 2010). On the other hand, PEG coated quantum dots showed reduced uptake by *Daphnia magna* and caused reduced inhibition of cell growth (Lewinski et al., 2010). Surface properties also influence aggregation, which is also one of the significantly important elements for toxicological evaluation of nanomaterials (Van Hoecke et al., 2011; Gosens et al., 2010). Brunner et al. (2006) revealed that insoluble nanoparticles significantly decrease cell activity and DNA content than hydrophilic nanoparticles.

2.2 Biology of Cyanobacteria

Cyanobacteria are gram-negative photosynthetic prokaryotes. They are widely distributed around world, and inhabit every environment. Over than 3500 millions of years old of cyanobacteria fossils have been found (Golubic and Seong-Joo, 1999). They seem to be evolutionarily related to chloroplasts in plants. They play an important role in the global bio-geo-chemical cycle by fixing carbon and nitrogen from the environment.

Photosynthesis and nitrogen fixation in cyanobacteria

Cyanobacteria are called blue-green algae because they contain the photosynthetic pigments chlorophyll-a and phycobilins. These pigments have characteristic optical absorption and fluorescence properties. In the simple prokaryotes, photosynthesis occurs directly in the cytoplasm, as opposed to in chloroplasts in higher photosynthetic organisms such as algae and plants. Photosynthesis is carried out through a set of light-dependent and light-independent reactions. In the light-dependent phase, carbon dioxide, water and sunlight are used as inputs to produce oxygen and energy, which is stored in the form of sugars. This energy is used for the light-independent process, the Calvin cycle.

The light-dependent process utilizes two reactive complexes, called photosystem I (PS I) and photosystem II (PS II), which is conserved in eukaryotic algae and in green plants. The two photosystems are associated with the electron transfer chain and are embedded in the thylakoid membranes of the cell. Phycobilins are the predominant energy collector in PS II (denoted P680). Chlorophyll-a is the predominant light absorbing pigments of PS I (P700). Each photosystem consists of a reaction center and the respective pigment molecules. First, the pigment molecules in P680 absorb a photon of the light and transfer it to an electron. The electron in the photosystem II is supplied by splitting water to produce oxygen and protons. The protons are pumped through ATPases in the thylakoid membrane to produce ATP. The photon-excited electrons are collected in the reaction center and transfer to P700 through electron transfer chain with loss of energy. When the electrons hit P700, they are further exited by another proton. These high energy electrons pass through electron transfer chain and effect redox reactions. NADP+ is reduced into NADPH. ATP and NADPH are used to make glucose in the Calvin cycle.

Cyanobacteria are also capable of nitrogen fixation. They can reduce free dinitrongen to ammonia via the nitrogenase enzyme. The fixed nitrogen is used for the synthesis of amino acids and nucleotides. There are two ways to by which nitrogen fixation is accomplished: organic and inorganic route. Proteins are broken down into amino acid via the organic route, while nitrates are reduced to nitrite and further to ammonia by the inorganic route. The process of reduction of nitrogen to ammonia requires 16 ATP as an energy source and proceeds according to the following reaction:

$N_2 + 16\ ATP + 8e^- + 8H^+ => 2NH_3 + 16\ ADP + 16\ P_i + H_2$

Cyanobacteria can be divided into three groups: the filamentous cyanobacteria with heterocysts (*Anabaena, Anabaenopsis, Aulosira, Calothrix, Nostoc*, etc…), the filamentous cyanobacteria without heterocysts (*Plectonema, Trichodesmium, Plectonema,* etc…) and unicellular cyanobacteria (*Syneccochoccus, Cyanothece, Gloeocapsa,* etc…). It was believed that filamentous cyanobacteria with heterocysts were the only species that do the nitrogen fixation. However, new studies have demonstrated that other groups of cyanobacteria can also do the nitrogen fixation in an aerobic environment (Carr and Whitton, 1982). Cyanobacteria without heterocysts and unicellular cyanobacteria also can fix nitrogen in aerobic condition during photosynthesis. *Syneccochoccus,* one of the unicellular cyanobacteria, is the example of an aerobic nitrogen fixing strain. Mitsui et al. (1986) studied nitrogen fixation and photosynthesis in different phases of the cell cycle of *Syneccochoccus,* and established that these two activities do not occur simultaneously. Cells are more likely do photosynthesis when oxygen evolution activity is high. The decrease of oxygen evolution activity induces the nitrogen fixation (Mitsui et al., 1986). *Cyanothece* is also capable of nitrogen fixation as well as photosynthesis. Reddy showed that nitrogenase of *Cyanothece* showed lower activity in the dark than in the light because of ATP generation.

Ion transport in cyanobacteria

Essential ions move in and out of cells by passive and active transfer processes. Passive transfer results from the difference in electrochemical potential maintained by the cell membrane. Passive diffusion of ions down a concentration gradient can occur across the lipid-bilayer membrane or through protein and ion channels. Active transfer is chemical interaction with carrier molecule, which requires the energy from ATP hydrolysis, and typically occurs against a concentration gradient. Additionally, ions have affinity with surface of cells. The cell surface is negatively charged; positively charged metal ions compete with other cations and replace them. Sulfhydryl group in the cell membrane can interact with metal ions to form S-metal-S bridges (Vymazal, 1987).

Cyanobacteria have distinct surface layers, which have unique molecular functional groups and metal binding properties. Yee et al. (2004) have shown that *Calothrix*, a filamentous cyanobacterium, has heterogeneously distributed metal binding sites on its

surface. Proton-active surface carboxyl, phosphoryl, hydroxyl, and amine functional groups located on the cell wall and exopolymer sheath interact with metal ions (Yee et al., 2004). Since this process is not ion-specific, along with essential ions, toxic ions also enter into the cell.

For resisting heavy metal ions toxicity, cyanobacteria possess heavy metal resistance systems. Metallothionein (MT), phytochelatins (PC) and polyphosphate bodies can sequester imbibed toxic metals. Metallothionein are low-molecular-weight, cysteine-rich, metal-binding proteins. Metal ions are sequestered in metal thiolate clusters of metallothionein. Metallothioneins are not only involved in detoxification of heave metals, they also play a role in Zn^{2+} homeostasis. Fowler classified metallothionein into three classes, class I, class II and class III (Fowler et al., 1987). Class I is polypeptides with locations of cysteine closely related to those in equine renal MT. Class II is polypeptides with locations of cysteine only distantly related to those in equine renal MT. Class III metallothioneins are atypical non-translationally synthesized metal-thiolate polypeptides (Turner and Robinson, 1995). The concentration of MT increases with the presence of heavy metal. PCs are enzymatically synthesized cysteine-rich peptides and structurally related to glutathione (GSH; g-Glu-Cys-Gly). They are active only in the presence of metal ions (Cobbett, 2000).

When heavy metal concentration is beyond detoxification limits, heavy metal ions damage the photosystem. The fluorescence of photosynthetic pigment changes as a result of the physiological stress (Dudkowiak et al., 2010). PS II seems to be more sensitive to heavy metal ions than PS I. Mercury damages the PSII reaction center and electron transfer chain (Lu et al., 2000). Sas et al. have shown that Cd also affects the transport electron chain of photosystem in *Synechocystis* and inhibit the activity of photosynthesis (Sas et al., 2006). In addition to the damage to the photosystem, toxic effects can also be observed in the morphology and ultrastructure of the cells. Rachlin studied morphological change of *Anabaena flos-aquae* and *Anabaena variabilis* after exposing the cultures to Zn in concentrations in excess of that required for the cells. With the increase in Zn concentration, both cells showed increased thylakoids and lipid bodies per cell (Rachlin et al., 1985). *Spirulina platensis* also showed similar results, but their thylakoid membranes were disorganized and had large intrathylakoidal spaces along with an increase in polyphosphate bodies after exposed to cadmium (Rangsayatorn et al., 2002). Phosphate, lipids, and

proteins bind positively charged heavy metal ions by electrostatic interaction (Vymazal, 1987). Additional studies by Surosz and Palinska (2004) show that the number and size of phosphate granules increase as the concentration of heavy metal ions increase. Rachlin et al. (1984) also reported that cadmium leads to an increase in the volume of polyhedral bodies, polyphosphate bodies, lipid inclusions, cyanophycin granules and membrane-limited crystalline inclusions in *Anabaena flos-aquae*.

Chapter 3. EXPERIMENTAL METHOD

3.1 Visualization of nanoparticles

Before exposing quantum dots to cells, size and fluorescence of quantum dots were characterized. Transmission electron microcopy (TEM) was used for size determination. No sample preparation was needed for TEM. Quantum dots were directly embedded on the grid and dried before measuring size. Fluorescence was measured to determine fluorescence changes before and after exposure to the culture.

3.2 Cells exposed to treatments and controls

Cell culture media (BG-11 media)

The trace metal mix consists of 2.86 g H_3BO_3, 1.81 g $MnCl_2{\cdot}4H_2O$, 0.222 g $ZnSO_4{\cdot}7H_2O$, 0.39 g $NaMoO_4{\cdot}2H_2O$, 0.079 g $CuSO_4{\cdot}5H_2O$, 49.4 mg $Co(NO_3)_2{\cdot}6H_2O$ with distilled water added to make up a total volume of 1 l. 1636.7 mg of BG-11 powder was purchased from Fluka (St. Louis, MO) and 1 ml of trace metal mix is added together in distilled water and adjusted in total volume of media as 1 l. The pH was adjusted at 7 using NaOH or H_2SO_4 and is crucial to obtain a desirable growth rate. Lastly, the media was autoclaved at 121°C for 15 m for sterilization.

Growth condition and culture preparation

Synnechococcus elongatus PCC 7942 (*Se*7942) culture was kindly provided by Professor Susan Golden of the University of California at San Diego. All the cultures were grown on an orbital shaker at 160 rpm, setting the temperature at 30 °C, with light intensity at 3000 lux as measured with a Davis light meter (Vernon Hills, IL). A master culture was prepared first either from freezer stock or a plated culture in BG-11 media. When the culture reached an optical density (OD) at 730 nm of 0.45, the master culture was readied for sub-culturing for further experimentation.

For every experiment, three replications of subcultures were prepared. 10 ml of master culture were added to 250 ml of fresh BG-11 media in 500 ml flasks, under growth

conditions. After samples reached OD_{730} of 0.1, subcultures were divided 25 ml each to 125 ml flasks without dilution for various treatments and controls.

The culture used for every experiment was prepared with the same method, as indicated above.

Various treatments and controls

Water insoluble quantum dots (WIQD): A core and shell structure of 5 mg/ml water-insoluble CdSe/ZnS quantum dots (WIQD) was obtained from Aldrich (St. Louis, MO), Cat. #694630. A hexadecylamine (HDA) ligand coating surface treatment was used for stabilization, and dots were dissolved in an organic solvent, toluene. The particle size is 3.4 nm and has a maximum excitation of 545 nm and emission at 560 nm, as indicated in company specifications. 4 mg/ml and 1 mg/ml of diluted quantum dots were prepared using toluene. Each concentration of WIQD was used to make 20 µg/ml (20 ppm) and 5 µg/ml (5 ppm), respectively, by adding 125 µl of each WIQD to 25 ml *Se*7942 culture.

Water soluble quantum dots (WSQD): A functional coating could prevent degradation and might have a different uptake mechanism. To verify the role of the functional coating, a carboxylic acid group with functionalized CdSe/ZnS quantum dots (WSQD) was obtained from Ocean Nanotech (Springdale, AR.), Cat. #QSH-580-04. It has a maximum emission of 580 nm with 4 nm particles size, as observed by TEM. 4 mg/ml of initial concentration of WSQD, which was diluted to 1 mg/ml to make a final concentration of 5 µg/ml (5 ppm) by adding 125 µl of 1 mg/ml diluted WSQD to *Se*7942 culture.

Cadmium control: Cadmium chloride $CdCl_2$ was obtained from Aldrich (St. Louis, MO) to differentiate the toxic effects of quantum dots and cadmium, which could be released following degradation. To make the same final concentration of cadmium with 20 ppm WIQD, inductively coupled plasma mass spectrometry (ICP-MS) was used to analyze the cadmium concentration in 20 ppm of WIQD culture media and arrive at the result that a 5 ppm cadmium concentration was in the 20 ppm WIQD. 125 µl of 1.63 mg/ml $CdCl_2$ were added to the 25 ml culture to make a final cadmium concentration of 5 ppm, equal to a Cd concentration of 20 ppm WIQDs.

Toluene controls (20 ppm and 5 ppm WIQD controls): To demonstrate whether the amounts of toluene used as solvent to disperse WIQDs is harmful to cultures, cultures were also exposed to the same amounts of toluene for dissolving WIQDs. 25 µl of toluene was used for 20 ppm WIQDs and 100 µl of toluene was used for 5 ppm WIQDs. 125 µl of WIQDs was added to the culture regardless of the final concentration, which means 5 ppm WIQDs used more toluene to dissolve than that of 20 ppm WIQDs.

Cadmium-Toluene controls: Not solely cadmium, but both cadmium and toluene could create a synergetic toxic effect. Both 100 µl of 2.04 mg/ml $CdCl_2$ and 25 µl toluene, which corresponds, to the Cd and toluene concentrations in the 20 ppm WIQD treatment, were added to the culture for a control setting.

3.3 Fate of quantum dots in cyanobacteria

Spectroscopic characterization

Optical density at 730 nm was measured as an indication of growth, and fluorescence scans from 350 nm to 600 nm for excitation range and 400 nm to 700 nm for emissions were measured for characterizing auto-fluorescence. A Tecan Infinite M200 spectrophotometer (Männedorf, Switzerland) was used for both optical density and fluorescence readings of samples at 6, 12, 18, 24, 36, 48, 60, 72 and 96 h after exposure to various treatments and controls.

Cell viability assay

SYTOX® Green assay consists of a dye that only penetrates plasma membrane of damaged or dead cells and attaches itself to the nucleic acid. It can be used for both gram-positive and gram-negative bacteria. The dye adhering to the nucleic acid after incubation emits fluorescence with excitation at 488 nm and emission at 530 nm. Flow cytometry or fluorescence spectroscopy is used for characterizing a cell population with this assay.

Cell membrane integrity is one way of determining cell viability. To conduct a live and dead cell assay, the commercial SYTOX® Green nucleic acid stain obtained from Molecular Probes, Inc. (Eugene, OR), Cat. #S7020, was used. To characterize the stain that

enters into damaged plasma membranes and chelates nucleic acids, emission at 530 nm with a 470 nm excitation source was used. 5 mM of SYTOX® Green was diluted to 0.25 mM using dimethyl sulfoxide (DMSO) and 0.4 µl of diluted stain was added to 200 µl of culture placed in a 96 well plate to make a final concentration of SYTOX® Green as 0.5 µM. Then, samples were incubated 10 m on an orbital shaker equipped in a fluorescence spectrometer to enhance the maximum reaction.

Solid media cultures

Solid media is also one way to determine cell viability reinforcing the result of a SYTOX® Green assay. To make a liquid BG-11 media into a solid, 12.0 g Bacto™ agar was mixed with 1636.7 mg BG-11 powder and 1 ml trace metal, to make a final volume of 1 l with distilled water. After adjusting a pH of 7.0 using NaOH or H_2SO_4, sterilization of media by autoclaving at 121 °C for 15 m was followed. Solidifying the BG-11 agar media in culture plates, 50 µl of samples 6, 12, 24 and 36 h after treatments were plated and kept at 30 °C, 3000 lux light intensity.

Does-response relationship

To find a certain minimum inhibitory concentration (MIC) of leaked cadmium below which there exists no significant toxicity to a cyanobacterial culture, cells were exposed to various concentration of cadmium. 1.63 mg/ml $CdCl_2$, the concentration used for cadmium control, was diluted by two-fold series dilution (1:2, 1:4, 1:8, 1:16, 1:32). 125 µl of each diluted solution was added to the 25 ml fresh culture as prepared by the same method as in the other experiments making a final cadmium concentration of 2.5 ppm, 1.25 ppm, 0.625 ppm, 0.312 ppm and 0.156 ppm. Every 24 hr, the growth and membrane integrity of cells were investigated.

Fluorescence flow cytometry

Flow cytometry is the technique for analyzing particles and cells in size of 0.2–150 µm using the principles of light scattering. When light of laser hit the particle or cells, it is scattering or diffracting in all angles. Magnitude of light scattered to forward is proportional to size of cells. Laser scattered by hitting cell granularity is called side scattering and determine cell granularity or internal complexity. It measures particle's relative size, relative

granularity or structural complexity, and relative fluorescence intensity. Cells are transported through a laminar stream across a laser source. The scatter from a passing cell is captured on a detector, optionally with the fluorescence from the cell. The fluidic system is structured so that only one cell passes through the laser beam at a time. The cell's membrane, nucleus and complexity of cell affect to the lighter scatter.

6, 12, 18, 24, 36, 48, 60, 72 and 96 h of all samples were analyzed via uptake of quantum dots and cell-level distributions of chlorophyll-A using flow cytometry. Quantum dots were characterized by 407 nm excitation and 585/42 emission filter, and cyanobacterial chlorophyll-A was examined by 633 nm excitation and 670/20 nm emission filter.

3.4 Uptake and distribution of quantum dots

Cell fractionation and inductively coupled plasma mass spectrometry (ICP-MS)

ICP-MS is a combination of inductively coupled plasma and mass spectrometer to determine the concentration of trace elements and the concentration of the elements in liquid and solid samples. The sample is aerosolized, and subsequently ionized by an argon plasma source. The mass spectrometer consists of a mass discrimination and detection system. First, the sample is aerosolized by mixing with argon gas and the aerosols undergo ionization by traveling different temperature zone of plasma. The positive ions are separated based on mass-to-charge ratio in mass spectrometer and only desired ions reached to detector. The detector generates a signal proportional to the concentration of the desired ions.

To determine the bio-distribution of cadmium within the cyanobacteria, inductively coupled plasma mass spectrometry (ICP-MS) was used. The procedure developed by Vallarta Jr. et al. (1998) was adapted for cyanobacteria and fractionated samples and samples without fractionation for cadmium analysis. First, 2 ml of cells which were exposed to CdSe quantum dots for 18 and 96 h, were centrifuged at 10,000 rpm (8,163 ×g) for 25 m. The Cd concentration in the supernatant was designated as fraction 1. The pellet was washed with 2 ml of distilled water to remove unbound quantum dots/cadmium on the surface of the cell. Then, it was centrifuged again for 5 m at 10,000 rpm, and the

supernatant of solution was called fraction 2. Fraction 1 and 2 were pooled together to analyze the cadmium concentration of the media. The washed pellet was re-suspended in 2 ml of 0.01 M ethylenediaminetetraacetic acid (EDTA) to remove cadmium bounded to the cell membrane and centrifuged at 10,000 rpm for 25 m. Supernatant from the centrifugation operation was called fraction 3, indicating Cd content in the cell membrane. The pellet was digested with 2 ml of a lysis buffer containing 50 mM Tris-HCl (pH 7.8), 0.3 mM MgSO4, 0.1 mM EDTA and sonicated for 5 pulses of 30 s with 75% power using a needle sonicator Model XL-2000 from Qsonica, LLC (Newtown, CT). The supernatant from centrifuging at 10,000 rpm for 25 m was collected as fraction 4, which corresponds to the intracellular Cd content. Unfractionated sample preparation was the same with the fractionated sample, but pools all of the fractions and cell debris in the tube. The difference between the Cd concentration of unfractionated and fractionated is the amount of Cd level in the cell debris.

Laser scanning confocal microscopy

Confocal microscopy was developed to overcome the drawback of optical fluorescence microscopy that produces blurry images. To create a high-resolution image by removing out-of-focus parts of an image, a pinhole is used to only pass in-focus light emission from a sample. By computationally combining a stack of in-plane 2D images, it is possible to reconstruct a three-dimensional image of the visualized object.

The brief mapping about the location of quantum dots and auto-fluorescence of cyanobacteria can be obtained by using a laser scanning confocal microscope from Leica Microsystems (Bannockburn, IL), Cat. #TCS SP2 RBB. 6 and 18 hr samples were mounted in a 2 % low melt agarose made with distilled water. TD 488/543/633 was used as a dichroic beamsplitter, and a 514nm Ar/HeNe laser was set at 90% power for excitation of both quantum dots and cholorophyll-A. The quantum dot emissions were measured from 580 to 600 nm (green channel) and the chlorophyll was auto-fluoresced at 660 to 680 nm (red channel). An image processing software program (ImageJ, http://rsbweb.nih.gov/ij/) was used to superimpose the false-color 2D image series and reconstruct 3D images.

Sample preparation for transmission electron microscopy (TEM)

An electron microscopy can provide visual information about structure, morphology and composition of biological materials and nanomaterials. Transmission electron microscopy (TEM) is used to measure the size of a nanoparticle and to visualize intracellular structures. Organism samples need varying degrees of preparation to preserve cell structure. Biological sample preparation is composed of processing, embedding and polymerization.

24 h treatment samples of WSQD and Cd were prepared for transmission electron microscopy according to the following procedure (Miller, 1982). Cell morphology was preserved using a microwave-based method as a primary fixation procedure. Samples were centrifuged at 4000 rpm with a micro centrifuge, Fisher Scientific (Pittsburgh, PA), Cat# 59A. Most of the supernatant was removed until it barely covered the samples. Samples were placed on ice for 30 s and microwaved at 90 s on, 20 s off and 9 sec on and again, placed on ice at 20 s. This process was repeated four times. To remove liquid from the samples, a cacodylate buffer (42.80 g Sodium Caqcodylate in 1000 Lwater) was used for washing. The washing step was repeated four times. For secondary fixation, 2 % (aq) OsO4 was added, enough to cover samples. Samples were placed on ice for 20 to 30 s and moved to a fresh water bath and microwaved twice for 9 s on, 20 s off, and 9 s on. Placing samples on ice and microwave steps were repeated five times for 5 m each. Then, they were incubated 5 m at room temperature. 3 % (aq) of KCN was added to samples with an equal volume of OsO4 added and incubated; samples were then rotated for 15 m without microwaving, followed by three repeated washings using purified water. After removal all water from samples, a filtered saturated uranyl acetate was added and microwaved for 9 s on, 20 s off and 9 s on, without chilling. Samples were covered and incubated for 30 m with rotation. The next step was dehydration. 10, 25, 50, 75, 95, 100 % of ethanol, a 1:1 mixture of 100 ethanol and acetonitrile, and pure acetonitrile were incubated, with 8 m of each. Infiltration has three sub-steps, a 1:1 mixture of acetonitrile and epoxy, 1:3 mixtures of acetonitrile and pure epoxy, and, finally, pure epoxy. Before adding new chemicals, chemicals in samples were removed. The first and second sub-steps had the same procedure. After adding mixtures, samples were vortexed and microwaved for 20 s and vortexed and incubated on the rotator for 10 m. Each of the sub-steps was repeated twice. For last sub-step, epoxy on the samples was removed and pure epoxy was added. Vortexing, microwaving for 30 s, vortexing, and

incubating on the rotator for 30 m all followed. Samples were replaced with fresh epoxy and incubated overnight. Finally, embedding and polymerizing were carried out. Mold was labeled and the tips filled with a drop of epoxy were prepared. Cultures were laid out to drain off and evaporate chemicals, but not with the intention for the culture to dry out. Samples were placed into the drop in the bottom of the mold well. The mold was filled with pure epoxy and placed in a Histodryer set at 85 °C, overnight. The next morning the blocks were cooled at room temperature before removing them from the molds. Images of cells were taken using TEM films and scanned by a DuoScan Scanner (AGFA Company).

3.5 Media contamination

Persistence assay

Fresh new samples of a 20 ppm WIQD treatment and cadmium-control and *Se*7942 were prepared. Waiting for cells death takes approximate two days, and then each culture was centrifuged at 4000 rpm for 10 m and separated into supernatant and pellet categories. To test cell viability, pellets from WIQD treated sample were mixed with 25 ml of new fresh BG-11 media, and pellets from the cadmium-treated sample were added to 25 ml of new BG-11 media. To test media contamination and its effect on new cells, pellets from fresh new health *Se*7942 were exposed to a supernatant of WIQD-treated culture and of cadmium-controlled culture, respectively. After all the combinations of damaged cells with fresh culture media and contaminated media with fresh culture pellets were applied, they were grown at 30 °C, 3000 lux of light intensity and shook at 160 rpm. Only OD at 730 nm was measured every 24 h.

Chapter 4. RESULT AND DISCUSSION

4.1 Characterization of quantum dots

Size and fluorescence of quantum dots were characterized before exposing to cells for verifying their properties measured by company. As seen in Figure 4-1, the size of quantum dots was in the range of 3 to 4 nm, regardless of hydrophobic and hydrophilic. The different dispersal mode of quantum dots was observed. Water insoluble quantum dots dissolved in toluene aggregated whereas water soluble quantum dots dispersed evenly. As product specification provided by company, hydrophobic and hydrophilic quantum dots have maximum excitation at 545 and 520 nm with emission at 560 and 580 nm respectively (Figure 4-2).

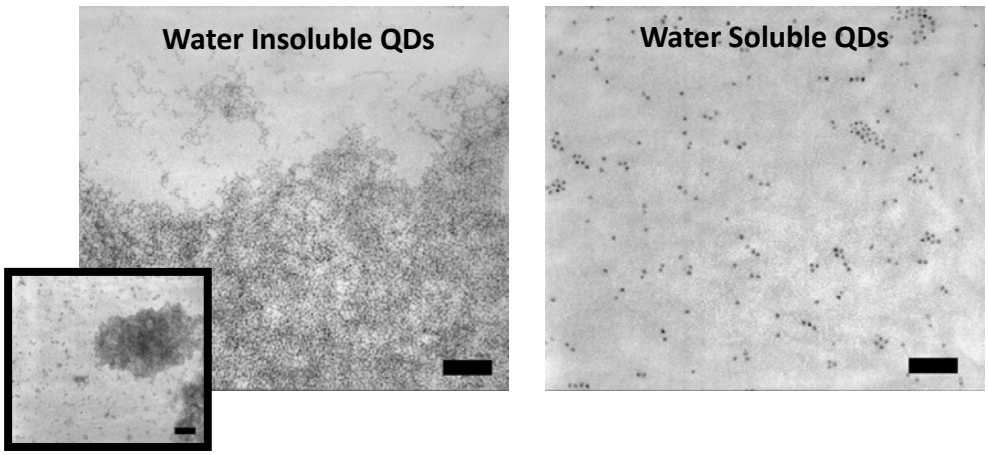

Figure 4-1. TEM visualization of quantum dots. Scale bar = 50 nm.

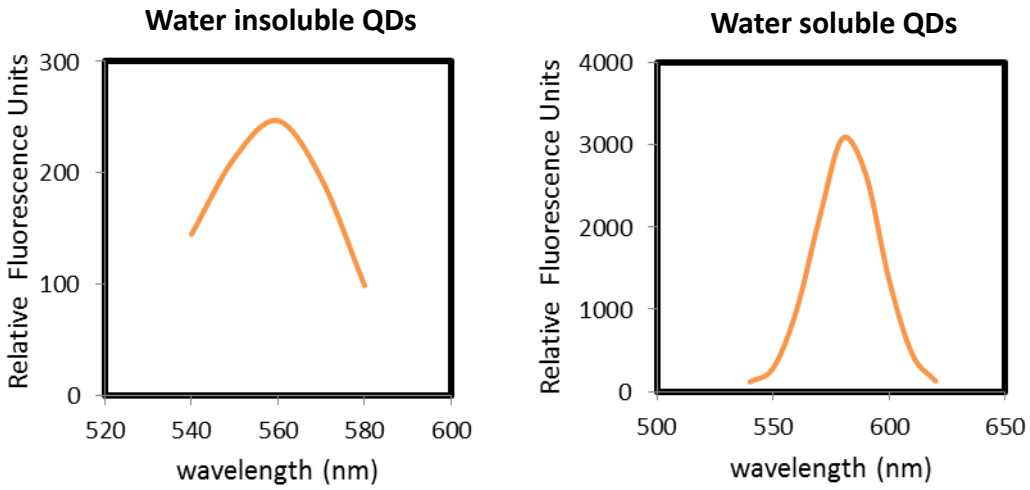

Figure 4-2. Fluorescence of quantum dots.

4.2 Fate of quantum dots in cyanobacteria

Impact on growth rate and cell viability

The growth curve is not a reliable measure for cell death itself, so the resulting graph of SYTOX® Green was plotted together in the Figure 4-3 for various treatments and controls. The fluorescence intensity from SYTOX® Green is proportional to the number of damaged and dead cells. The growth curve was divided into two parts since cultures have to grow to sufficient density for treatments. *Se*7942 was grown at 30 °C, 3000 lux and shaking at 160 rpm until the mid-exponential growth phase, around 1.0 of OD_{730}. At this point (t=0), the culture was exposed to various treatments. Figure 4-3 (A) and (B) are to differentiate quantum dots toxicity and cadmium toxicity, by-product of quantum dots degradation. As seen in the Figure 4-3 (A), little growth inhibition was observed for the toluene control for 20 ppm WIQDs compared to untreated *Se*7942 control. 20 ppm WIQDs treated cells have the highest growth inhibition rate compared to cells with other treatments. 20 ppm WIQDs treatment, cadmium and cadmium-toluene controls not only inhibited cell growth but also did kill the cells. Cadmium-toluene control showed similar toxic reactions to the WIQDs

treatments which was a more acute inhibition than cadmium itself. In Figure 4-3 (B), trends of SYTOX® Green assay are corresponding to growth rate. Toluene control seemed to have almost no effect on destabilizing the membrane compared to *Se*7942 control. Numerous cells treated to 20 ppm WIQDs were dying within 6 h exposure and showed the highest membrane destabilization kinetics. Even cadmium-toluene control showed lower cell membrane destabilization than WIQDs treatment, it seemed that combination of toluene and cadmium showed summative effect to the growth inhibition. Figure 4-3 (C) and (D) are to elucidating the effect of factional coating on quantum dots toxicity. The growth inhibition and cell membrane damage results for 5 ppm WIQDs treated cells were similar to 20 ppm WIQDs treated cells. The carboxylic acid group of 5 ppm WSQDs had no toxic effects on the cells, which was the opposite result of the same concentration of 5 ppm hydrophobic quantum dots or similar toluene levels (Figure 4-3 (C)). Hydrophilic quantum dots did not seem to have any effect on the cell membrane and remained alive while 5 ppm hydrophobic quantum dots and toluene both showed cell membrane damage. Note that the amount of toluene in toluene control for 5 ppm WIQDs is four times larger than that in toluene control for 20 ppm WIQDs (Figure 4-3 (D)).

To reinforce the membrane damage results of SYTOX® Green assay, 6, 12 24, 36 h post exposure cells with various treatments and controls were plated on solid media and their growth on plates are shown in Figure 4-4. Even though cultures remain their original color (Figure 4-6), no cell growth on plates was observed for 6 hr exposure cells treated with WIQDs and cadmium-toluene. Cadmium treated cells have longer lifetime than WIQDs and cadmium-toluene control, which stopped growing after 12 h exposure. Thus, Figures 4-3 and 4-4 both demonstrated cell membrane damage after treated with WIQD and cadmium and decreased cell growth as a result of cell death.

Since cadmium and WIQDs showed similar cell growth inhibition rate and viability at both 20 ppm and 5 ppm, it was assumed that the threshold for cadmium toxicity was far lower than what the cells were treated with. To determine the threshold cadmium concentration, cell cultures were subjected to decreasing cadmium concentrations. From the growth inhibition assay, the threshold of cadmium concentration was determined to be between 0.313 ppm (1:16 dilution) and 0.156 ppm (1:32 dilution) which was 10 times smaller than concentration of cadmium control (Figure 4-5).

Photographs of culture flasks were taken to observe the color change of cultures exposed to various treatments and controls over several time intervals (Figure 4-6). We observed that photosynthetic pigments faded over time and shifted towards cyan in color. This might be due to the fact that different pigments have their own degradation rate or that each pigment possesses different adaptive responses to stress (Prasad et al., 1991). WIQD treatment and cadmium-toluene control lost their color completely after 36 h exposure.

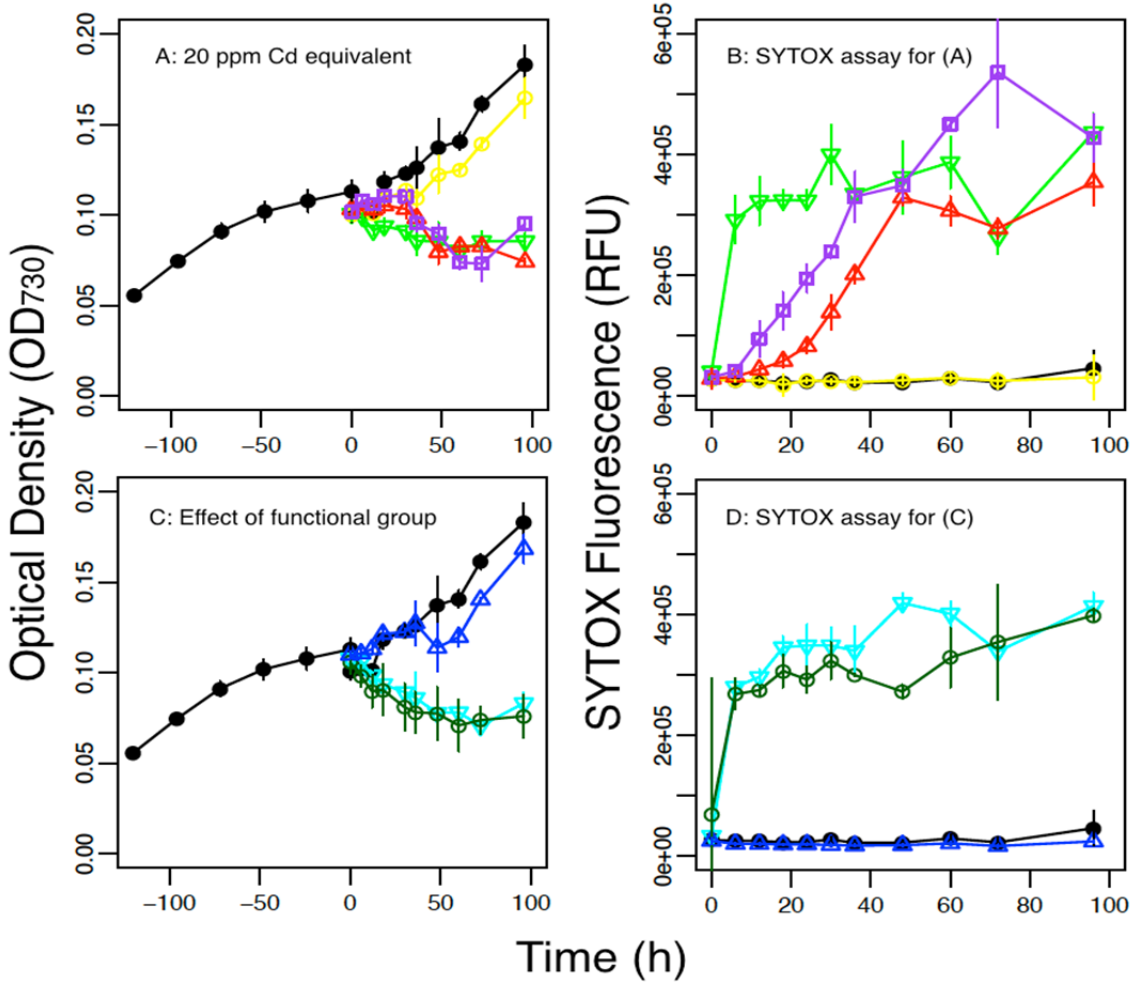

Figure 4-3. Growth rate and cell viability of *Se*7942 with various treatments and controls. Untreated *Se*7942 control (●) *Se*7942 + 20 ppm WIQD (▽) Toluene control for 20 ppm WIQD (○) Cadmium control (△) Cadmium-Toluene control (□) *Se*7942 + 5 ppm WIQD (▽) Toluene control for 5 ppm WIQD (○) *Se*7942 + 5 ppm WSQD (△).

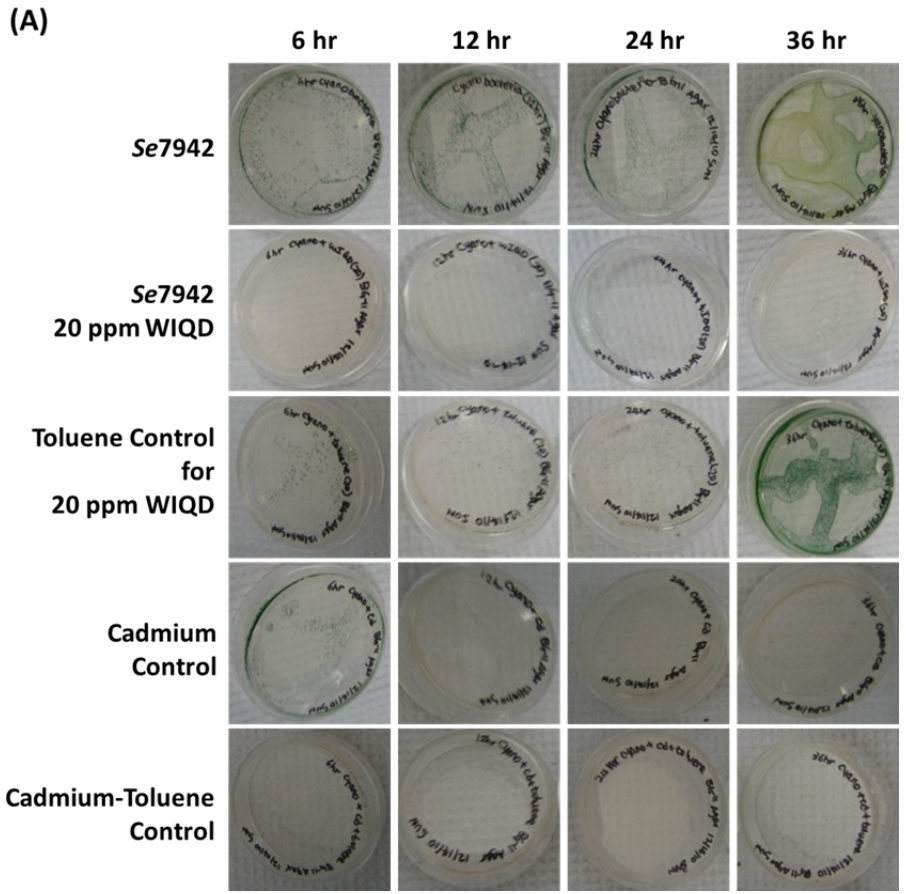

Figure 4-4. Photographs of solid culture plates for various treatments and controls. (A) The results were similar to the SYTOX assay; water insoluble quantum dots had the lowest cell viability than other samples. Even with 6 h exposure, water insoluble quantum dots lost their viability while the cadmium control lost their viability after 12 h exposure.

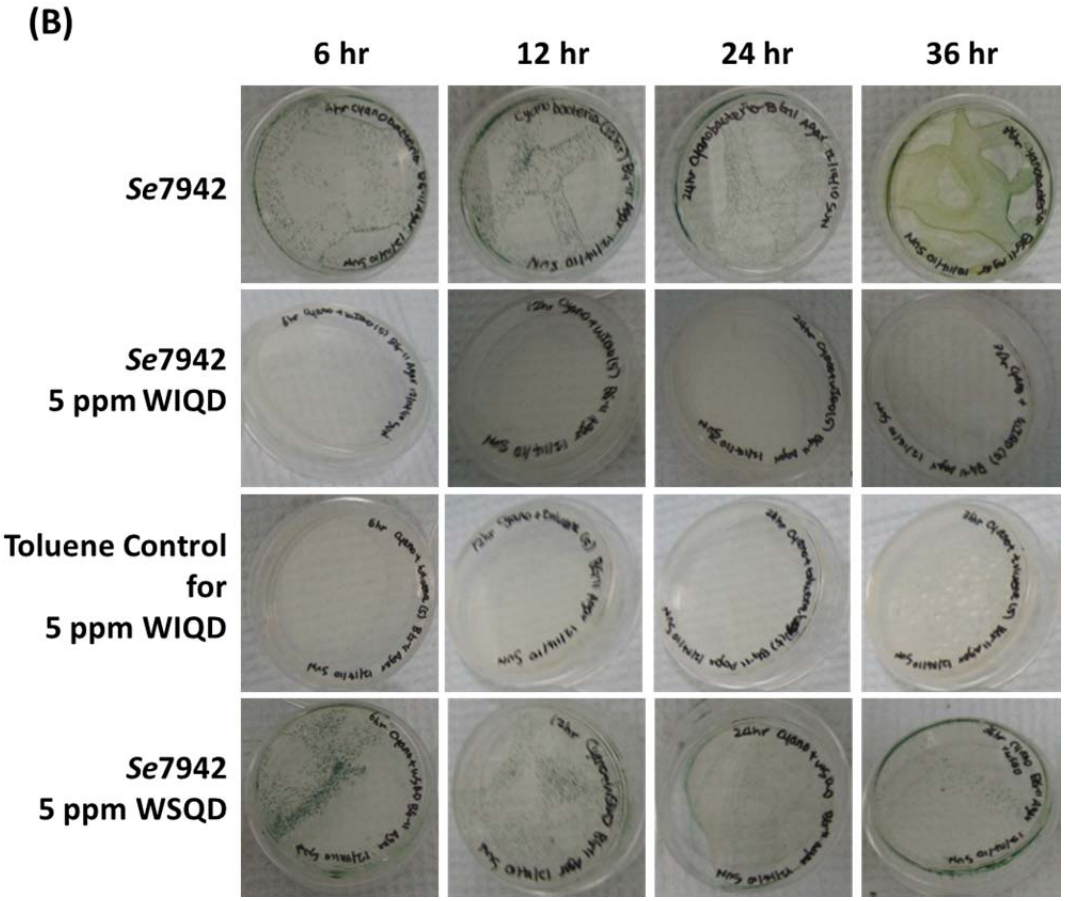

Figure 4-4 (continued). (B) Unlike water insoluble quantum dots, water soluble quantum dots did not lose their viability.

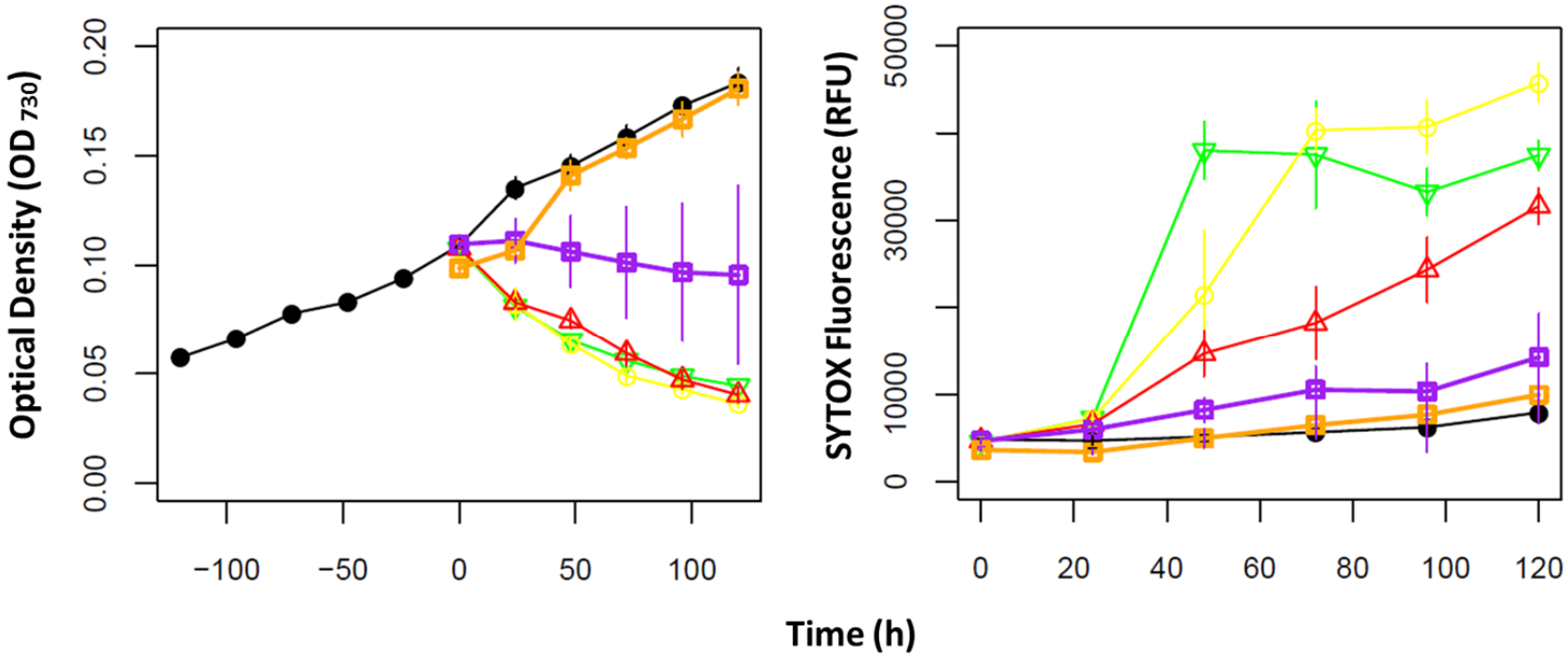

Figure 4-5. Dose-response relationship. Untreated *Se*7942 control (●) 2.5 ppm Cadmium (1:2 dilution) (▽) 1.25 ppm Cadmium (1:4 dilution) (○) 0.625 ppm Cadmium (1:8 dilution) (△) 0.313 ppm Cadmium (1:16 dilution) (□) 0.156 ppm Cadmium (1:32 dilution (□).

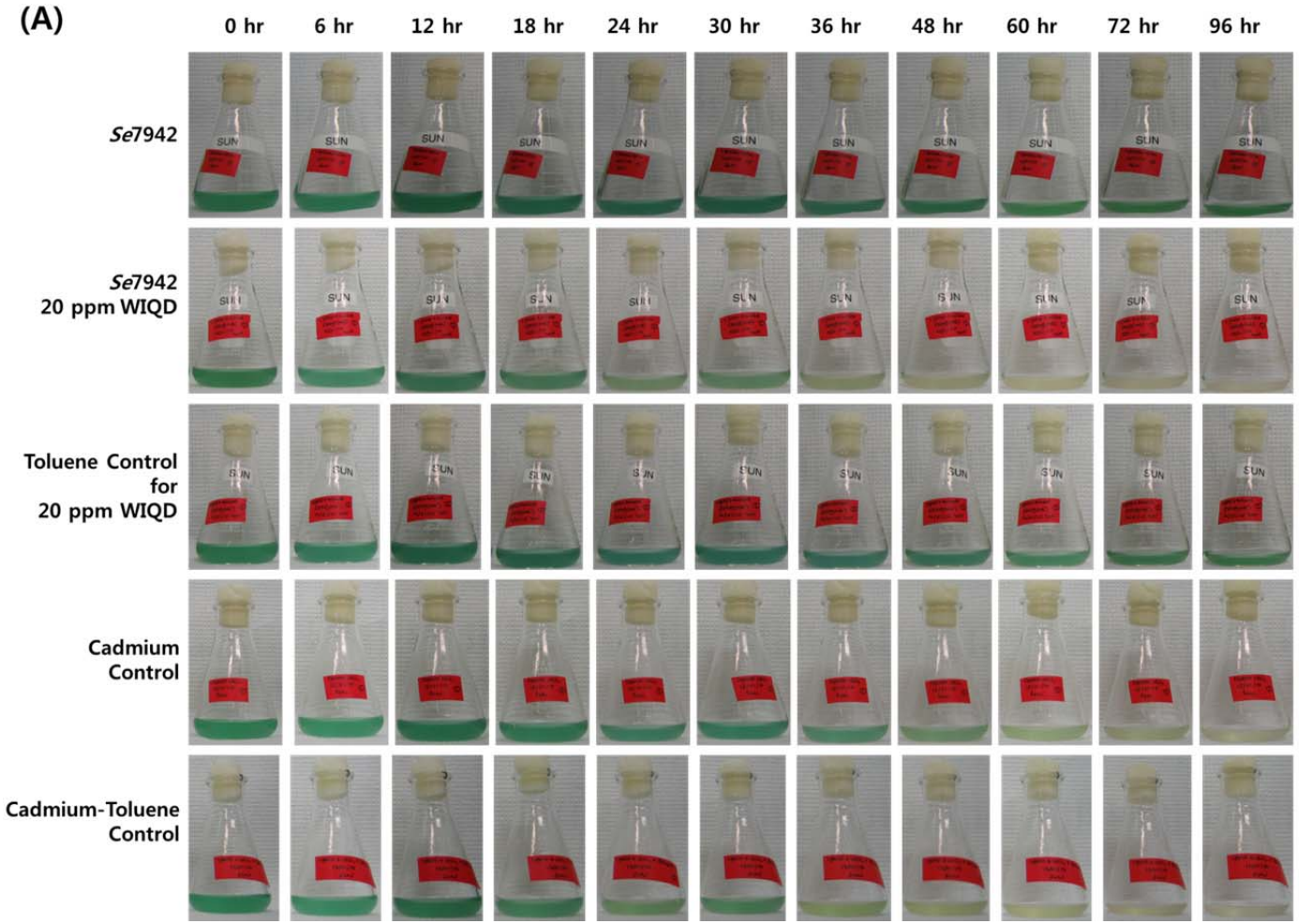

Figure 4-6. Photographs of flasks for various treatments and controls over several interval exposure intervals. (A) Photosynthetic pigments of WIQDs and cadmium containing cultures faded over time.

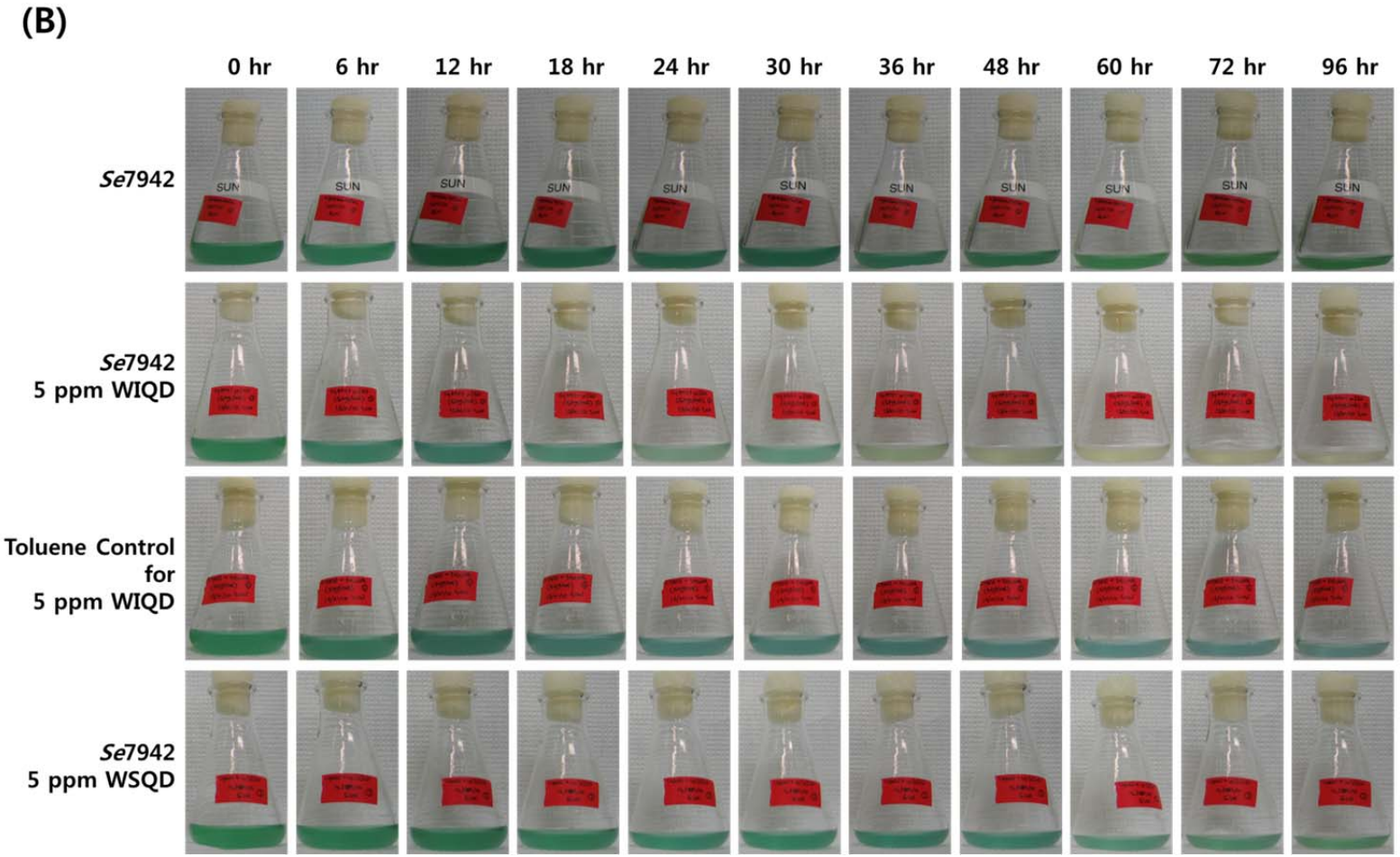

Figure 4-6 (continued). (B) Toluene control culture changed their color toward cyan. Cells treated WSQDs were observed to have similar color as cells with no treatment.

Measurement of photosynthetic pigments

The change in color due to cadmium and WIQDs exposure, and the destabilization of the membrane could indicate a display of specific modes of toxicity to photosynthesis. We collected the samples exposed to various treatments and controls for analyzing fluorescent photosynthetic pigments and the cadmium uptake kinetics. As another photosynthetic reaction system, *Se*7942 was also composed of photosystems I and II (denoted PSI and PS II) which are connected by an electron transfer chain to capture solar energy to produce chemical energy of adenosine triphosphate (ATP) and reduced form of nicotinamide adenine dinucleotide phosphate (NADPH). Phycobilin, chlorophyll-A and carotenoids are key pigments that charge the photosynthesis of cyanobacteria and are embedded in intracellular structures called thylakoid membranes (Colyer et al., 2005). PS II is where phycobilin is the predominant pigment as an energy collector which first absorbs the solar light and excites electrons. The exited electrons lose their energy via an electron transfer chain and finally hit the reaction center of PS I where chlorophyll-A is the predominant light-absorbing pigment. The chlorophyll-A fluorescence intensity is determined by the redox state of the PS II electron acceptor. chlorophyll-A fluorescence decreases if the electron flow from the donor side in the PS II reaction is inhibited. When the electron flow from to the acceptor side in the PS II reaction inhibits, the fluorescence of chlorophyll-A is increased (Sudhir et al., 2005; Carr and Whitton, 1973; Carr and Whitton, 1982).

The 2-D spectrum aids in viewing all of ancillary pigments the information participating in the photosynthesis process even though chlorophyll-A is characterized by 680 nm fluorescence emission. An excitation bandwidth from 350 nm to 600 nm and emission bandwidth from 400 nm to 700 nm in 10 nm steps are used for a 2-D spectrum fluorescence matrix (Figure 4-7).

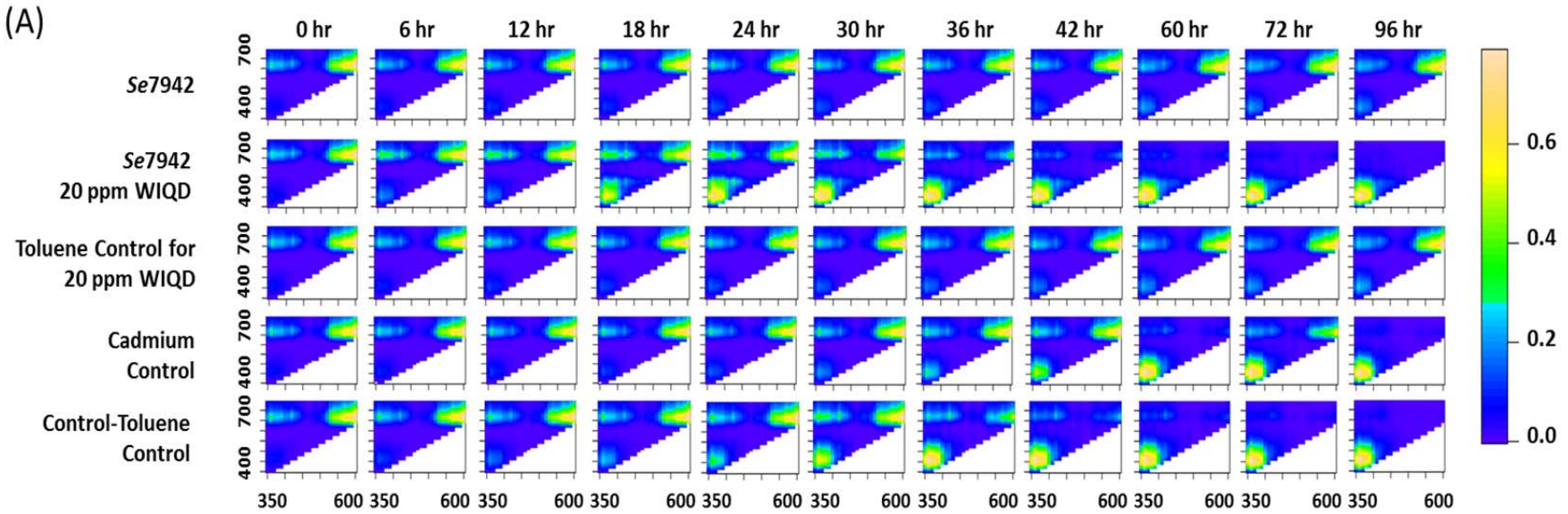

Figure 4-7. Fluorescence matrix for characterizing the overall toxic effect on photosynthesis pigments. (A) Data were normalized to the highest peak of chlorophyll-A at 450 nm, which did not change after various treatments and controls. Cadmium containing samples showed the fluorescence of photosynthesis pigments changing results which differed from the toluene controls.

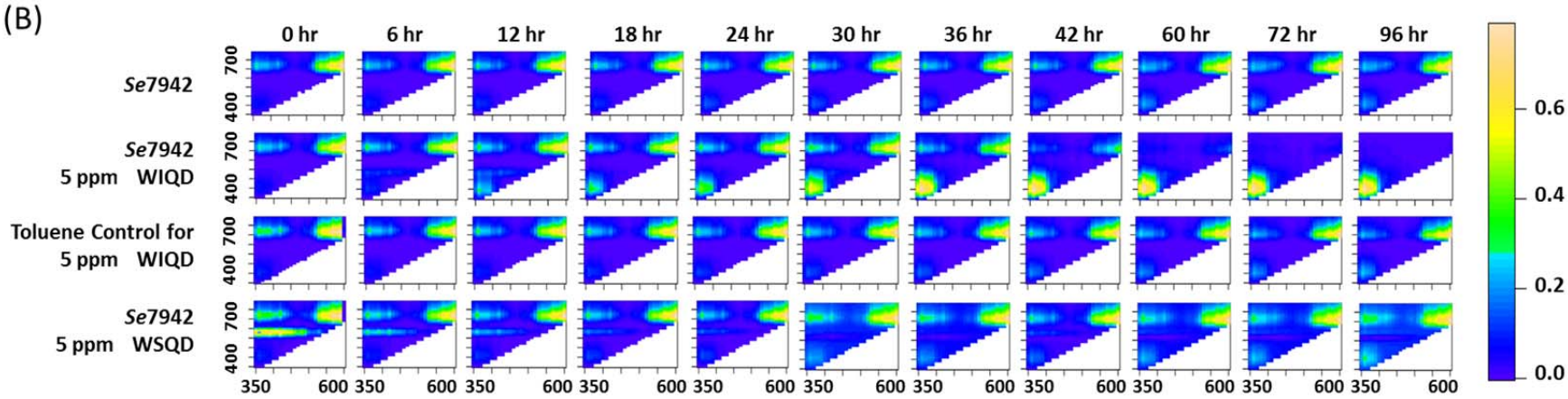

Figure 4-7 (continued). (B) The peak around emission 450 nm appeared after 30 h exposure of WSQDs.

Data for the fluorescence matrix were normalized by the fluorescence emission of chlorophyll-A around 450 nm, which did not seem to be affected much by various treatments and controls. Chlorophyll-A (PS I), which has a fluorescence emission peak around 680 nm, decreased over time indicating a loss in functionality of photosystems. As seen in Figure 4-7, when cells were coping with stress, the peak of pigment fluorescence changed. Novel peaks were only in the emission around emission 650 nm with fluorescence matrix of intact photosystem but they disappeared and new peaks appeared in the around emission 450 nm with the fluorescence matrix of a damaged photosystem. The behavior of fluorescence pigments changed in WIQDs and cadmium treated cells in that a novel peak roughly around 450 nm was appeared, which demonstrated that the electron transport activity of photosystems was decreasing. Toluene toxicity to photosynthetic pigments was lower than cadmium toxicity. Interestingly, the toluene control for 5 ppm WIQDs, where a higher amount of toluene was added than the control for 20 ppm WIQDs, showed cell membrane destabilization but had less of an effect on the photosynthetic systems. Small peaks in the emission 450 nm in the matrices in both toluene controls could be a result of the small amount of degradation of pigments, which might induce the culture color shift towards cyan as we observed in the photographs of flasks. Unlike WIQDs, the WSQDs themselves maintained their fluorescence until 18 h post-exposure, confirmed by a broad absorption and narrow emission range around 580 nm. Even though the broadband of WSQDs fluorescence might not be the same as the fluorescence of WSQDs by themselves due to the normalized data, it faded out and disappeared after 24 h exposure, indicating that they may have degraded or were photobleached by light. The degradation of QDs could affect the photosystem of cyanobacteria since the peak around emission 450 nm seemed to appear after the loss of the fluorescence broadband of WSQDs. The peak around emission 450 nm in the matrix could suggest that cadmium released from WSQDs after degradation could affect photosystems.

To characterize levels of chlorophyll-A on a per-cell basis, a 633 nm excitation and 670/20 nm emission filter of flow cytometry was used. Figure 4-8 is corresponding to the fluorescence matrix that 20 and 5 ppm WIQD treatments, cadmium control and cadmium-toluene control lost their auto-fluorescence in a very short time. WSQDs treatment did not affect auto-fluorescence distribution over time.

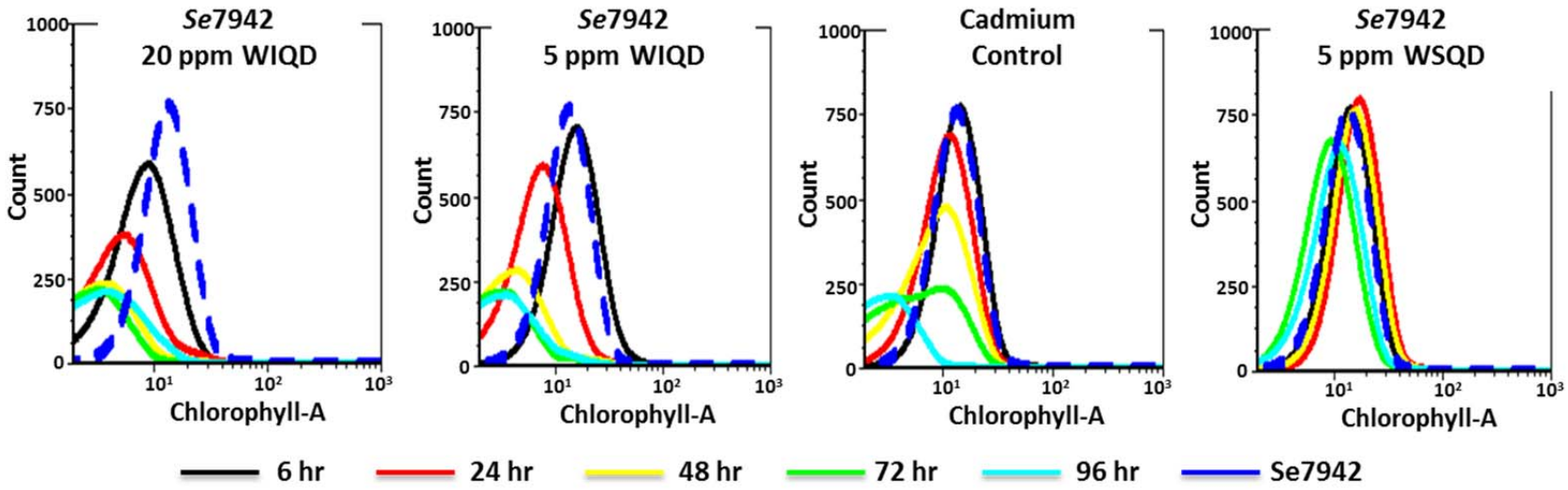

Figure 4-8. Characterization of cell basis chlorophyll-A distribution by flow cytometry. Only water soluble quantum dots treated cells did not change to chlorophyll-A distribution but other cells lost their auto-fluorescnece. Even cadmium control cells changed their chlorophyll-A distribution and became same as water insoluble quantum dots at 96 h, having a slower rate of change than hydrophobic quanutm dots.

Flow cytometry was used not only for characterizing distribution of chlorophyll-A on a per cell basis but also for morphological changes within a cell. Composed of forward and side scatter patterns gives morphological information about cells since the size of the cells is proportional to the magnitude of forward scatter, and granularity and structural complexity of cells are represented by side scatter. The scatter plot showed an interesting result that seemed to come from instrument error at first glance but it was not. Only cadmium containing samples showed two distinct subpopulations while WSQD culture continuously formed as one population (Figure 4-9). The appearing subpopulation corresponded to Figure 4-8. When the relative cell number became below 580 and fluorescence intensity of chlorophyll-A became lower in Figure 4-8, the so-called threshold value, the subpopulation appeared in scatter plot. We could not find any information to explain this peculiar observation. However, the results suggested that the WIQDs, and cadmium treated cells changed their granularity and structural complexity. Despite the toluene treated cells changed their chlorophyll-A color to cyan, the cell basis chlorophyll-A distribution and scatter plot differed little from the untreated *Se*7942.

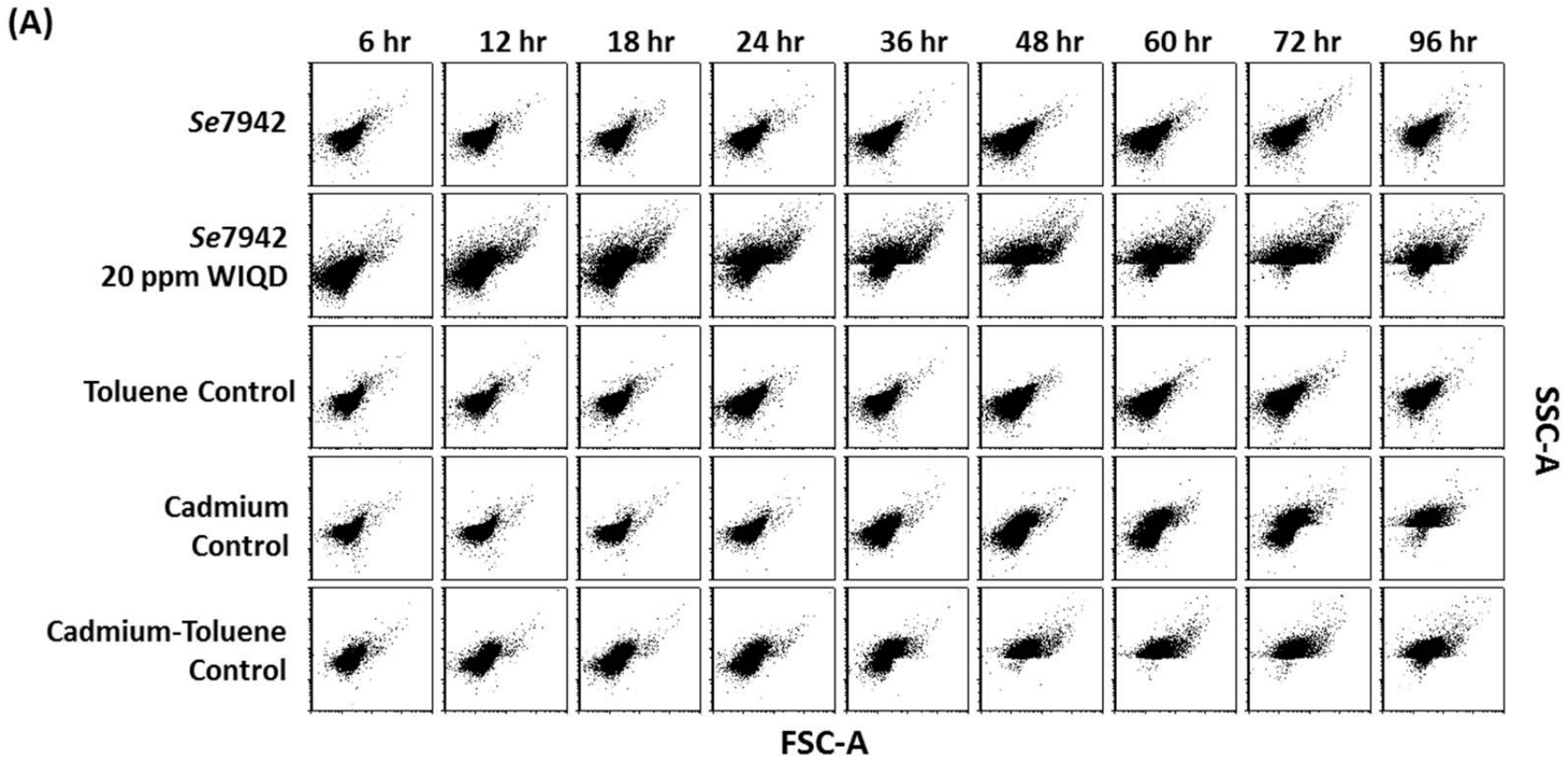

Figure 4-9. Characterization of morphological change by forward and side scatter plots of flow cytometry data. (A) Cadmium containing cultures showed two distinct subpopulations.

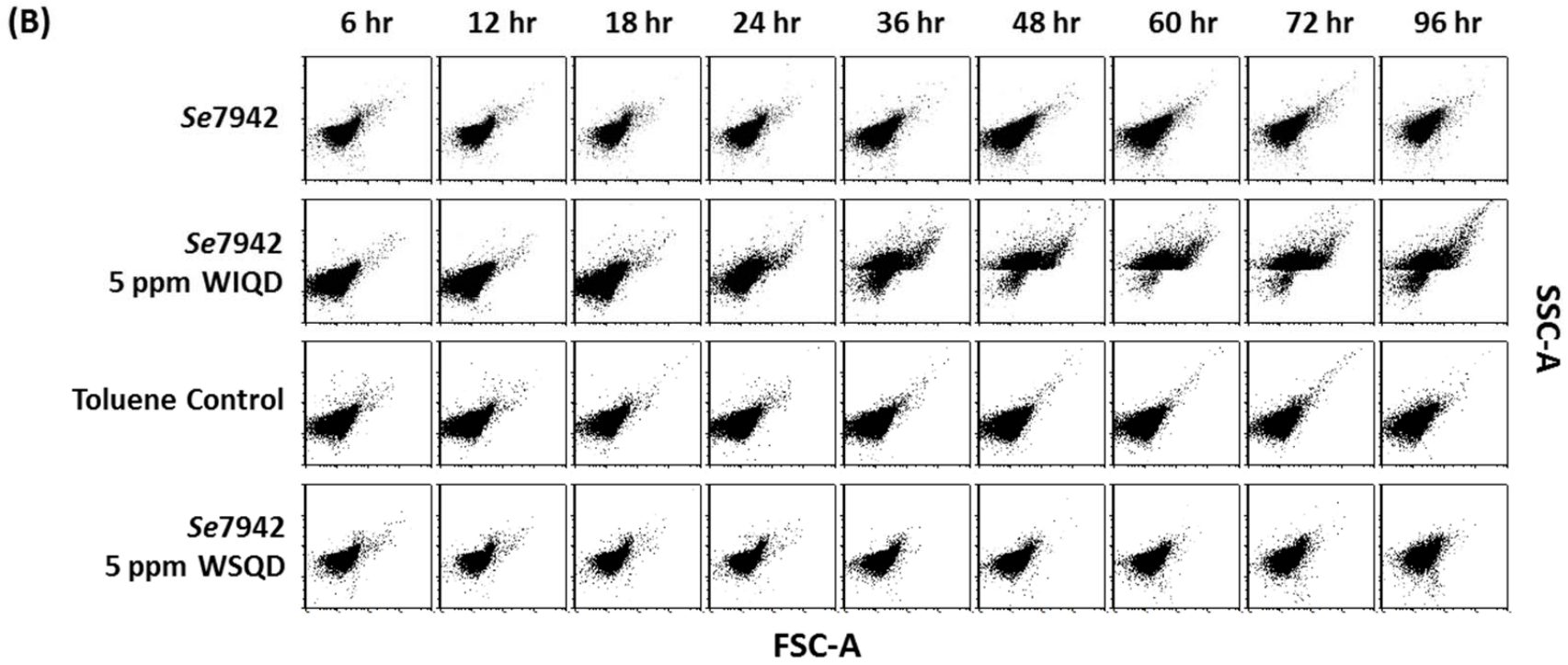

Figure 4-9 (continued). (B) Cells exposed to WSQDs continuously remained in one population.

4.3 Degradation rate of quantum dots

Degradation of CdSe/ZnS quantum dots

Previous observations indicated that cadmium and quantum dots possess similar consequence of toxic effects to cells. The degradation rate of the quantum dots could be main key element to result toxicity in cyanobacteria since cells showed no toxic responses to WSQDs which kept as intact structure due to carboxylic acid groups. The degradation of samples of WSQDs in BG-11 media, WIQDs dissolved in toluene and WIQDs in BG-11 media was compared in Figure 4-10, measured after 5 m of sample preparation (all the samples are 5 ppm concentration). WIQDs dissolved in toluene were still in intact form but WIQDs in BG-11 media degraded and lost their fluorescence rapidly within 5 m. WSQDs had the highest fluorescence, which suggests that the surface coating maintains the photostability of quantum dots and increases quantum yields.

WSQDs photostability was observed over long period time by fluorescence spectroscopy (Figure 4-11). WSQDs in BG-11 media was incubated in the same condition as culture growth environment, at 30 °C, light intensity at 3000 lux and shaking at 160 rpm. After 96 h, the fluorescence of WSQDs remained their fluorescence and increased it due to media evaporation, indicating surface coating determine the degradation rate of quantum dots and their toxicity. Hydrophilic quantum dots with surface coating are non-toxic substance. However, leaking cadmium after degradation determines the toxicity of cyanobacteria as we observed. Thus, surface coating of WSQDs is an important key point in predicting ecological toxicity.

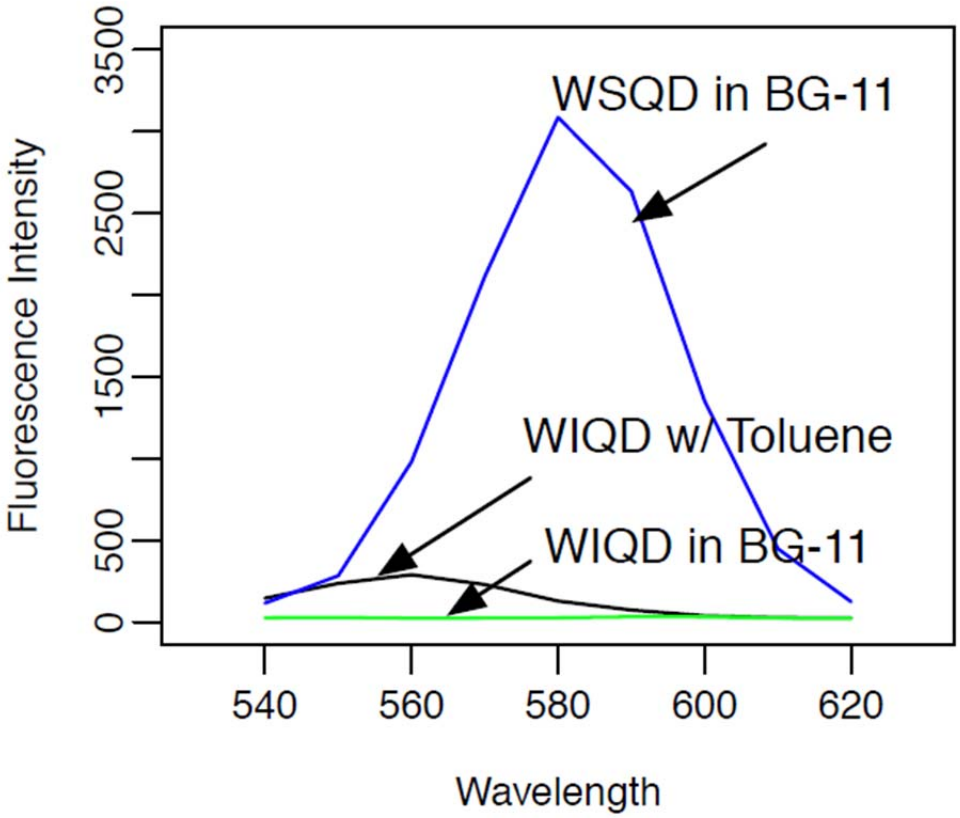

Figure 4-10. Degradation of quantum dots. No fluorescence of WIQDs in BG-11 media was detected maybe because of light and hydrophobic and hydrophilic interaction. WSQDs in BG-11 media showed highest photostability. 20 ppm WIQDs in toluene ▬ 20 ppm WIQDs in culture media ▬ 5ppm WSQDs in culture media ▬.

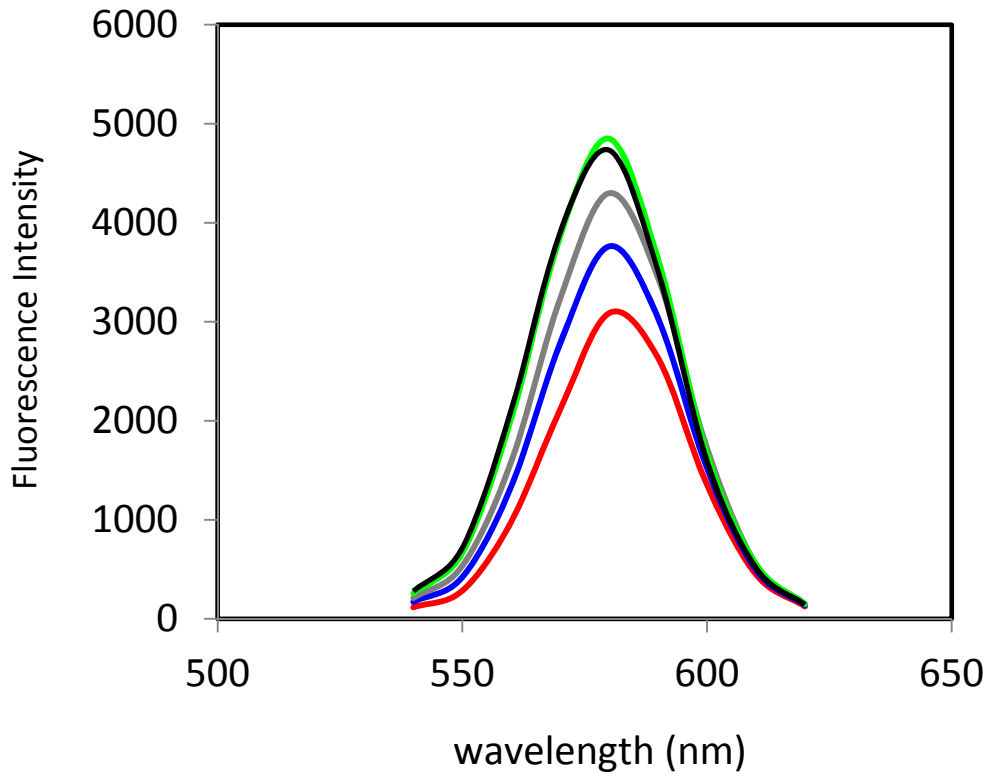

Figure 4-11. Stability of water soluble quantum dots in BG-11 media. WSQDs was incubated in the same condition as culture growth environment at 30 °C, light intensity at 3000 lux and shaking at 160 rpm. WSQDs had peak at 580 nm and it was increased over time. 0 h — 24 h — 48 h — 72 h — 96 h —.

4.4 Uptake and distribution of quantum dots

Quantum dot / cadmium uptake in Se7942

The potential uptake route and distribution of quantum dots and cadmium within the cyanobacterial cells were analyzed. There are two processes for metal uptake by cells: passive and active transport process. Passive transport process involves interaction of metals and cell wall, and passive diffusion whereas active transport process involves energy dependent active metabolic reaction. Endocytosis is known as the common way for nanoparticles entering into cells. Not much prior information is available about mechanism of water insoluble quantum dots uptake by cyanobacteria since previous researches more focus on size and surface charge dependent endocytosis (Verma and Stellacci, 2010). Several studies on heavy metal toxicity especially cadmium resistance have been researched in freshwater cyanobacterium, *Microcystis aeruginosa* (Zeng et al., 2009; Zeng and Wang, 2009). Cd^{2+} ions are sequester by binding to negative surface of polyphosphate, lipid and protein, by interacting with sulphydryl groups to produce –S-metal-S bridges and by interacting with thiol groups of class Ⅱ metallothioneins (Vymazal, 1987; Olafson et al., 1979; Baptista and Vasconcelos, 2006)**.** Cd^{2+} ions are also sequestered in phyto chelation and polyphosphate bodies which acting as detoxifying mechanism (Vymazal, 1987). In the case of WSQDs with a carboxylic acid group, surface coating of WSQDs could conjugate with lipid components on the cell membrane or with carboxylic acid of fatty acid on cell wall, and finally enter into cells through endocytosis or macropinocytosis (Zhang and Monteiro-Riviere, 2009; Chang et al., 2006).

To investigate approximate location of quantum dots in cells, inductively coupled plasma mass spectroscopy, flow cytometry and laser scanning confocal microscopy were used. Results of flow cytometry and laser scanning confocal microscopy are plotted in Figure 4-12 and 4-13. Quantum dots distribution in the cell population was examed by 407 nm excitation and 585/42 emission filter of flow cytometry (Figure 4-12). A maker (M1) was set since changes were seen at the left side of x-axis. WIQDs treated cells were not distinguishable from Cd controlled cells, confirming no WIQDs were uptake by cells due to rapid degradation of WIQDs.

As has been noticed previous sections and in a literature (Dashdorj et al., 2004), Cd ions and WIQDs damaged photosystems causing a shift in the fluorescence spectrum. Both flow cytometry and confocal microscopy images verified the increase number of cells in the emission range of 570 to 590 nm as a result of damaging photosystems. Green channel, 570 to 590 nm emissions, represented QDs and red channel represented cells' auto-fluorescence in Figure 4-13. The intensity of both channels has been increased by image process software to distinguish with background. WIQDs themselves were invisible at any wavelength in or on cells, but green channel was same shape as red channel in WIQDs treated cells confirming a shift in fluorescence spectrum. Cadmium control sample also showed an auto-fluorescence spectrum shift. Data of flow cytometry was gated at 585 nm for quantifying self-assembled quantum dots to cell and fluorescence spectrum shift by nanoparticles (Table 4-1). In the case of WIQDs, the value is proportional to the photosystem damaged cells since WIQDs were not observed after exposure. Less population of cells exposed to 5 ppm WIQDs was that of 20 ppm WIQDs, indicating dose-response uptake kinetics that lower concentration of WIQDs less damage photosystems.

In the case of WSQDs, size of 1 to 2 μm aggregated quantum dots were merged in the cell membrane (Figure 4-13). As seen in Table 4-1, proportion of cells taken up WSQD was relatively constant at around 20 % over time.

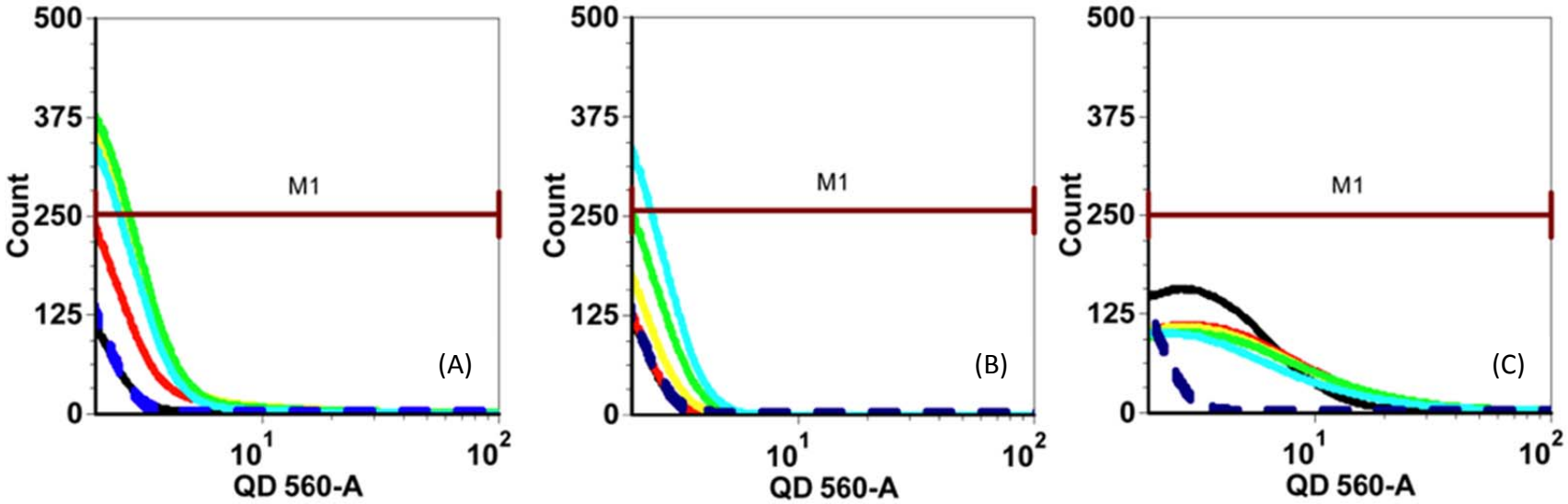

Figure 4-12. Quantum dots and Cd uptake measured by flow cytometry. (A) *Se*7942 + 20 ppm WIQD. Quantum dots were not observed in the cells. (B) Cadmium control. Results of cadmium controlled cells were similar with WIQDs treatment. (C) *Se*7942 + 5 ppm WSQD. 6 h — 24 h — 48 h — 72 h — 96 h — *Se*7942 —.

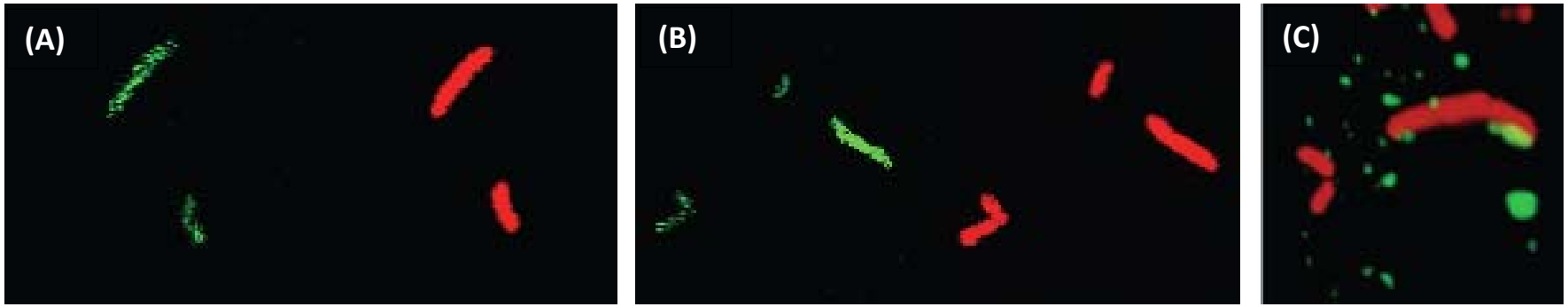

Figure 4-13. Confocal microscopy image of quantum dots and Cd. (A) *Se*7942 + 20 ppm WIQD. Green channel showed similar shape as red channel indicating that photosystem was damaged by quantum dots. (B) Cadmium control. Results of cadmium controlled cells were similar with WIQDs treatment. WIQDs and Cd ions damaged photosynthesis pigments and shift cells' auto-fluorescence emission. (C) *Se*7942 + 5 ppm WSQD. Aggregated WSQDs were merged in the cell membrane. Green channel emission = 570 to 590 nm. Red channel emission = 660 to 680 nm.

Table 4-1. Quantifying the percentage of cells gated by 585/42 emission filter.

	Control	6 hr	12 hr	18 hr	24 hr	36 hr	48 hr	60 hr	72 hr	96 hr
*Se*7942 + 20 ppm WIQD	1.44	2.22	4.6	6.93	9.73	13.81	18.81	19.48	20.73	16.18
*Se*7942 + 5 ppm WIQD	1.44	2.18	1.7	3.76	3.04	11.9	13.74	15.76	14.05	14.39
*Se*7942 + 5 ppm WSQD	1.44	23.03	25.46	22.57	20.74	18.97	20.42	20.01	19.75	17.22

In the case of WIQDs, the percentage represents the photosystems damaged cells. 20 ppm WIQDs showed higher kinetic rate of percentage of the damaged cell than 5 ppm WIQDs. In the case of WSQDs, the percentage represents the proportion of cells taken up WSQDs, which was relatively constant over time.

Biodistribution and kinetics (ICP/MS)

To characterize localization of cadmium in the culture, WIQDs, WSQDs treatments and cadmium control samples were fractionated into cell media, cell membrane, intracellular and cell debris. Cd content of each compartment was measured by ICP-MS over two different exposure time, 18 and 96 h. Cd content in media, cell membrane, intracellular content and cell debris were compared in Figure 4-14. Level of Cd in cell debris is the difference between the unfractionated sample and the sum of other fractions (cell media, cell membrane and intracellular and represents the unaccounted amounts of cadmium. The assumption for WIQDs treated cells was that Cd contents represent not intact WIQDs but only Cd ions that released from core part of quantum dots after degradation since no fluorescence of WIQDs was detected by flow cytometry and confocal microscopy. The assumption for WSQDs treated cells was that Cd contents mostly composed of intact WSQDs since fluorescence of WSQDs remained consistently, but high temperature argon of ICP-MS degraded intact WSQDs into cadmium. To compare Cd content for 18 and 96 h samples, data were normalized with biomass and calculated as percentage since media evaporation was observed over time that Cd content in total sample increased. As seen in Figure 4-14, Cd contents self-assembled with cell membrane increased over time in all cases. In case of WIQDs treatments and cadmium controls, cadmium was continuously sequestered in cell membrane by passive transport process despite cells lost their viability. Unlike other samples, Cd levels of intracellular increased in cells exposed to WSQDs since quantum dots were taken up by live cells continuously. WSQDs were more effectively uptake by cells for several reasons. Cells exposed to WSQDs showed limited toxicity and functional coating of intact quantum dots could do self-assemble with cell membrane. Lastly, several mechanisms were available for cadmium degraded form quantum dots. However, WIQDs uptake mechanisms only limited to the last mechanisms of sequestering leaked cadmium.

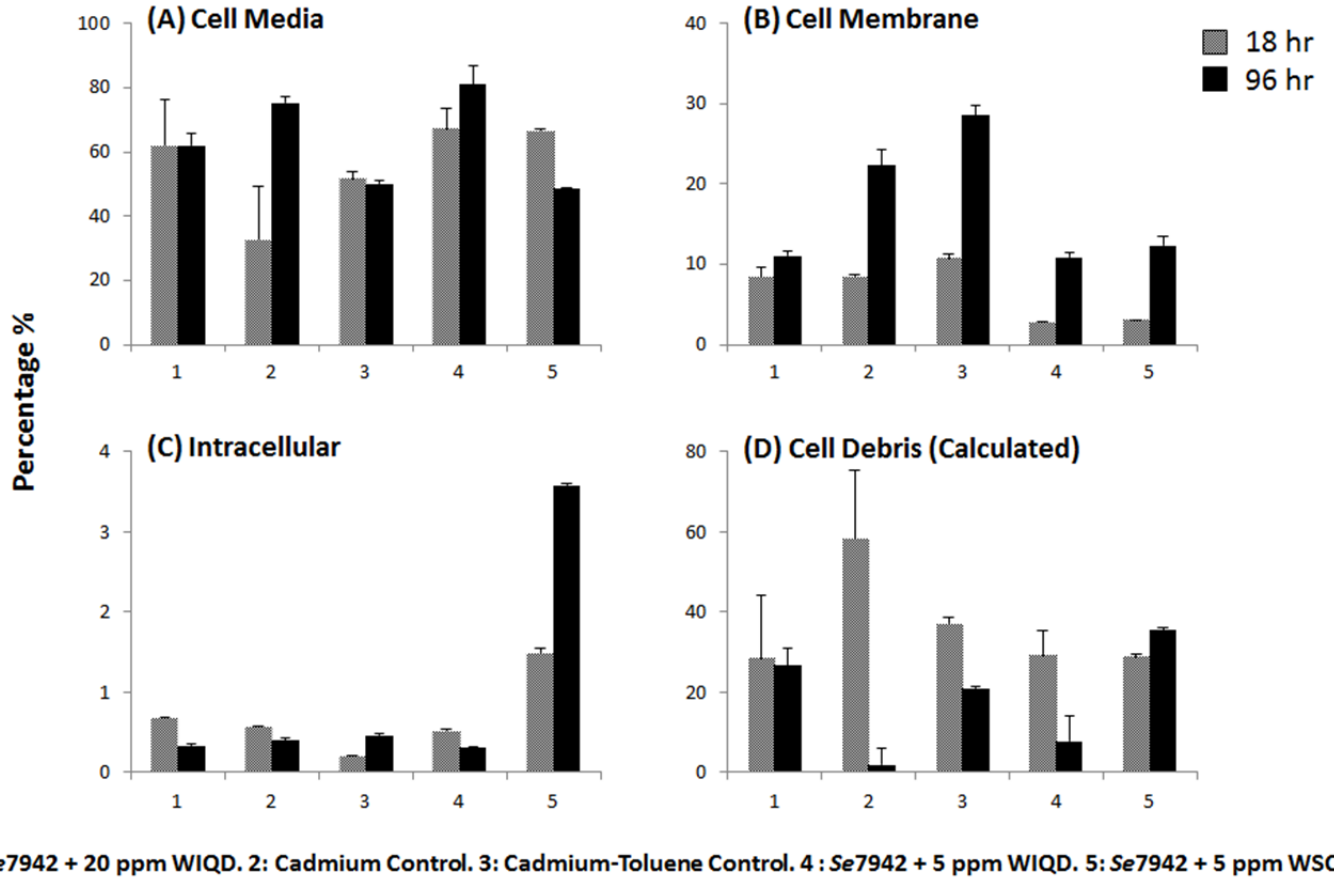

Figure 4-14. Comparison of cadmium content over time in fractionated samples. (A) Cd content in cell media. (B) Cd content on cell membrane. (C) Cd content in inside the cell. (D) Cd content in cell debris (calculated).

Visualization of intracellular structure using transmission electron microscopy

Intracellular structures of cells exposed to untreated *Se*7942, 20 ppm WIQDs treatment, cadmium control and 5 ppm WSQDs treatment were visualized after 24 h exposure by transmission electron microscopy (Figure 4-15). Cd ions seem to affect directly to phosphate bodies which provide a storage site for essential metals acting as a detoxifying mechanism (Seufferheld et al., 2008). Some phosphate bodies in cadmium control cells were torn out entirely, possibly because of polyphosphate degradation which could induce loss of cell viability (Nishikawa et al., 2003). Phosphate bodies in WIQDs were not torn out but they had lighter color than *Se*7942. We are not sure why cadmium control gives more stress to phosphate bodies than WIQDs treatment but this detoxification mechanism might help to prevent acute toxicity in terms of viability. In the image of cells treated WSQDs, dark lipid globules aggregated on the cell wall. We presume that a carboxylic acid group of WSQDs makes chemical bond with fatty acid on edge of cell wall.

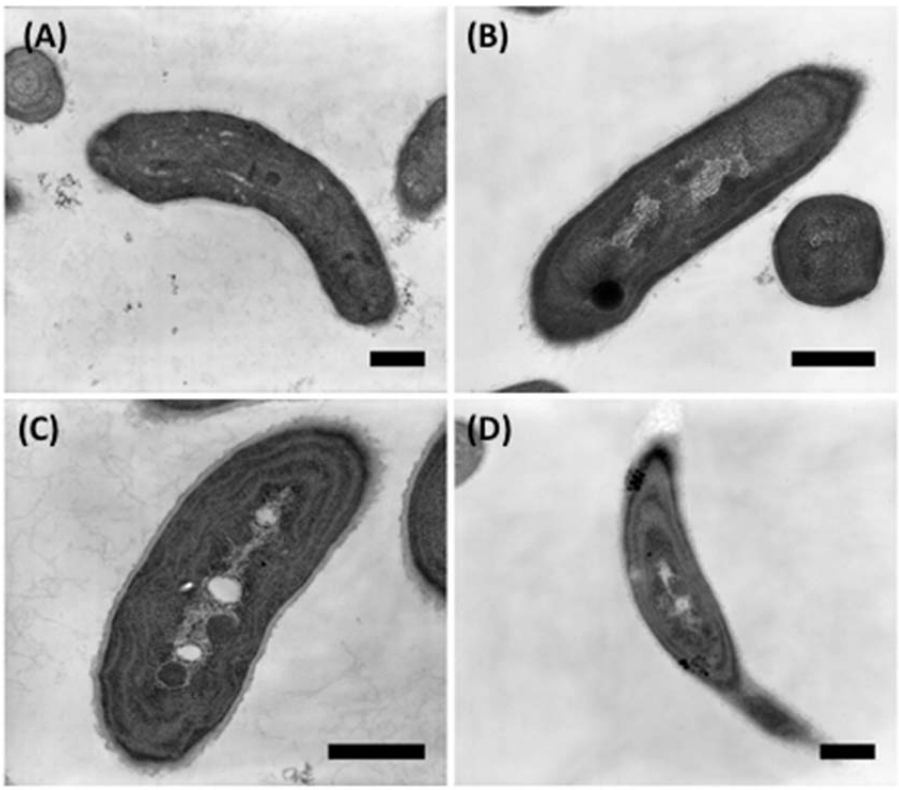

Figure 4-15. Ultrastructure of cells with different treatments. (A) Untreated *Se*7942. (B) *Se*7942 + 20 ppm WIQD. (C) Cadmium control. (D) *Se*7942 + 5 ppm WSQD. Scale bar = 0.5 micron.

Persistence assay

Life cycle of nanoparticles in the environment has recycle and redispersion potential, which differentiates environmental mobility of nanoparticles from that of the life cycle in the human bodies. Here, we tested recycle and redispersion to elucidate further information for life cycle and secondary impact in the environment. Damaged cells did not grow in new fresh media which confirmed results of viability assays. Growth of fresh cells in contaminated media was inhibited and photosynthesis pigments lost their color, which is similar to the result of WIQDs treatments or cadmium controls (Figure 4-16 and 4-17). Once cadmium leaked from quantum dots releases to aqueous system, they can have further harmful effect to new health organisms.

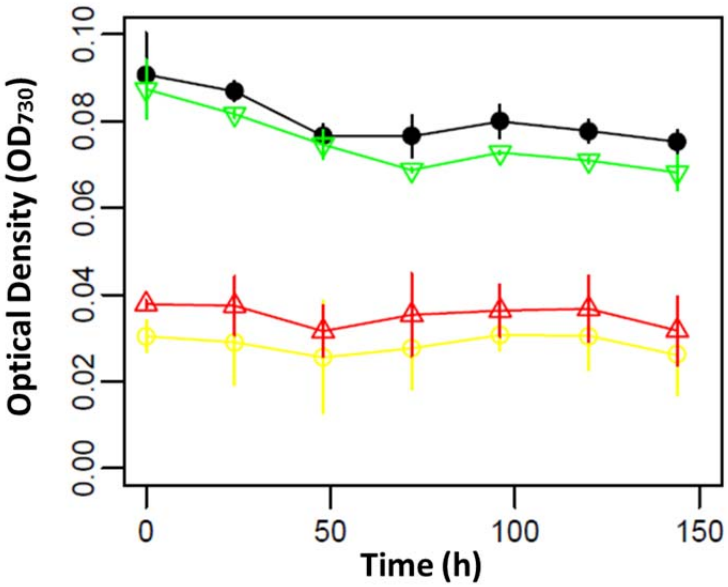

Figure 4-16. Cells growth for persistent assay. Dead cells did not grow at all and new live cells die in contaminated media. Fresh BG-11 media + WIQD treated pellet — Fresh BG-11 media + Cd treated pellet — WIQD treated media + *Se*7942 pellet — Cd treated media + *Se*7942 pellet —.

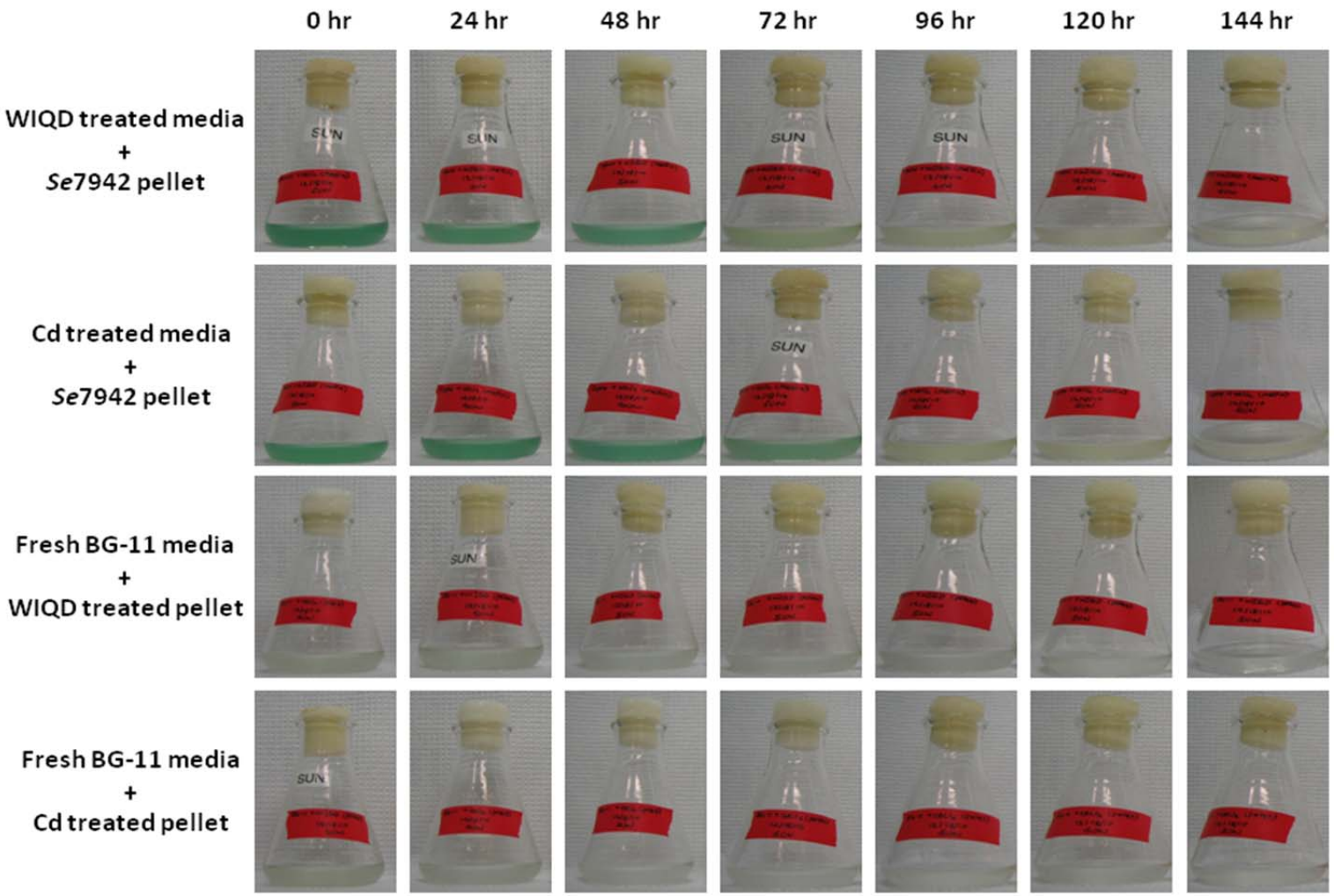

Figure 4-17. Photographs of flaks for persistence assay.

Chapter 5. CONCLUSION

In this study, CdSe/ZnS quantum dots and cyanobacterial species were chosen for evaluating potential fate of nanoparticles in the environment. Surface coating and degradation rate of quantum dots were two main factors of determining their toxicity to cyanobacteria. Aggregated WSQDs were self-assembled to the cell membrane and continuously taken up by cyanobacteria via passive and active transport mechanisms. However, WSQDs had no effect to cell growth and viability at the concentration tested since surface coating of a carboxylic acid group on WSQDs kept quantum dots intact, preventing cadmium released from a core portion of quantum dots. WIQDs, quantum dots without protection of surface coating, were vulnerable to light and were easily degraded into cadmium and selenium. Thus, toxic responses of quantum dots were similar to that of cadmium, indicating most quantum dots toxicity was governed by leaked cadmium ions. WIQDs were impacting the photosynthetic machinery of the cyanobacteria resulting in a shift of auto-fluorescence spectrum. We also characterized toxicity of toluene, the solvent to suspend water insoluble quantum dots. Even though cell exposed to only toluene changed in color observable to the naked eye, their auto-fluorescence was not different with respect to untreated *Se*7942. To characterize elimination/recycle of nanoparticles for comprehensive understanding quantum dots life cycle in the environment, media contamination was analyzed. Contaminated media from quantum dots showed further toxic effect in new health cells. The result indicates that quantum dots have to be handled carefully to not disperse into environment.

REFERENCES

Adams, L. K., D. Y. Lyon and P. J. J. Alvarez. 2006. Comparative eco-toxicity of nanoscale TiO2, SiO2, and ZnO water suspensions. *Water research* 40(19): 3527-3532.

Archibald, J. M. 2009. The Puzzle of Plastid Evolution. *Current Biology* 19(2): R81-R88.

Auffan, M., J. Rose, J. Bottero, G. V. Lowry, J. -. Jolivet and M. R. Wiesner. 2009. Towards a definition of inorganic nanoparticles from an environmental, health and safety perspective. *Nature Nanotechnology* 4(10): 634-641.

Bagalkot, V., L. Zhang, E. Levy-Nissenbaum, S. Jon, P. W. Kantoff, R. Langery and O. C. Farokhzad. 2007. Quantum dot-aptamer conjugates for synchronous cancer imaging, therapy, and sensing of drug delivery based on Bi-fluorescence resonance energy transfer. *Nano Letters* 7(10): 3065-3070.

Baptista, M. S. and M. T. Vasconcelos. 2006. Cyanobacteria metal interactions: Requirements, toxicity, and ecological implications. *Critical reviews in microbiology* 32(3): 127-137.

Blaser, S. A., M. Scheringer, M. MacLeod and K. Hungerbühler. 2008. Estimation of cumulative aquatic exposure and risk due to silver: Contribution of nano-functionalized plastics and textiles. *Science of the Total Environment* 390(2-3): 396-409.

Braydich-Stolle, L. K., N. M. Schaeublin, R. C. Murdock, J. Jiang, P. Biswas, J. J. Schlager and S. M. Hussain. 2009. Crystal structure mediates mode of cell death in TiO2 nanotoxicity. *Journal of Nanoparticle Research* 11(6): 1361-1374.

Brayner, R., S. A. Dahoumane, C. Yéprémian, C. Djediat, M. Meyer, A. Couté and F. Fiévet. 2010. ZnO nanoparticles: Synthesis, characterization, and ecotoxicological studies. *Langmuir* 26(9): 6522-6528.

Brunner, T. J., P. Wick, P. Manser, P. Spohn, R. N. Grass, L. K. Limbach, A. Bruinink and W. J. Stark. 2006. In vitro cytotoxicity of oxide nanoparticles: Comparison to asbestos, silica, and the effect of particle solubility. *Environmental Science and Technology* 40(14): 4374-4381.

Carr, N.G. and B.A. Whitton. 1973. *The biology of blue-green algae*. University of California Press.

Carr, N.G. and B.A. Whitton. 1982. *The biology of cyanobacteria*. University of California Press.

Chang, E., N. Thekkek, W. W. Yu, V. L. Colvin and R. Drezek. 2006. Evaluation of quantum dot cytotoxicity based on intracellular uptake. *Small* 2(12): 1412-1417.

Chithrani, B. D., A. A. Ghazani and W. C. W. Chan. 2006. Determining the size and shape dependence of gold nanoparticle uptake into mammalian cells. *Nano Letters* 6(4): 662-668.

Cobbett, C. S. 2000. Phytochelatins and their roles in heavy metal detoxification. *Plant Physiology* 123(3): 825-832.

Coe, S., W. Woo, M. Bawendi and V. Bulović. 2002. Electroluminescence from single monolayers of nanocrystals in molecular organic devices. *Nature* 420(6917): 800-803.

Colyer, C. L., C. S. Klinkade, P. J. Viskari and J. P. Landers. 2005. Analysis of cyanobacterial pigments and proteins by electrophoretic and chromatographic methods. *Analytical and Bioanalytical Chemistry* 382(3): 559-569.

Conner, S. D. and S. L. Schmid. 2003. Regulated portals of entry into the cell. *Nature* 422(6927): 37-44.

Dashdorj, N., W. Xu, P. Martinsson, P. R. Chitnis and S. Savikhin. 2004. Electrochromic Shift of Chlorophyll Absorption in Photosystem I from Synechocystis sp. PCC 6803: A Probe of Optical and Dielectric Properties around the Secondary Electron Acceptor. *Biophysical journal* 86(5): 3121-3130.

Derfus, A. M., W. C. W. Chan and S. N. Bhatia. 2004a. Intracellular delivery of quantum dots for live cell labeling and organelle tracking. *Advanced Materials* 16(12): 961-966.

Derfus, A. M., W. C. W. Chan and S. N. Bhatia. 2004b. Probing the Cytotoxicity of Semiconductor Quantum Dots. *Nano Letters* 4(1): 11-18.

Dudkowiak, A., B. Olejarz, J. Łukasiewicz, J. Banaszek, J. Sikora and K. Wiktorowicz. 2010. Heavy Metals Effect on Cyanobacteria Synechocystis aquatilis Study Using Absorption, Fluorescence, Flow Cytometry, and Photothermal Measurements. *International Journal of Thermophysics*1-12.

Dumas, E., V. Ozenne, R. E. Mielke and J. L. Nadeau. 2009. Toxicity of CdTe quantum dots in bacterial strains. *IEEE Transactions on Nanobioscience* 8(1): 58-64.

Fowler, B. A., C. E. Hildebrand, Y. Kojima and M. Webb. 1987. Nomenclature of metallothionein. *Experientia.Supplementum* 5219-22.

Gao, X., L. Yang, J. A. Petros, F. F. Marshall, J. W. Simons and S. Nie. 2005. In vivo molecular and cellular imaging with quantum dots. *Current opinion in biotechnology* 16(1 SPEC. ISS.): 63-72.

Golubic, S. and L. Seong-Joo. 1999. Early cyanobacterial fossil record: Preservation, palaeoenvironments and identification. *European Journal of Phycology* 34(4): 339-348.

Gosens, I., J. A. Post, L. J. J. de la Fonteyne, E. H. J. M. Jansen, J. W. Geus, F. R. Cassee and W. H. de Jong. 2010. Impact of agglomeration state of nano- and submicron sized gold particles on pulmonary inflammation. *Particle and Fibre Toxicology* 7.

Hagemann, M. 2011. Molecular biology of cyanobacterial salt acclimation. *FEMS microbiology reviews* 35(1): 87-123.

Hardman, R. 2006. A toxicologic review of quantum dots: Toxicity depends on physicochemical and environmental factors. *Environmental health perspectives* 114(2): 165-172.

Hauck, T. S., R. E. Anderson, H. C. Fischer, S. Newbigging and W. C. W. Chan. 2010. In vivo quantum-dot toxicity assessment. *Small* 6(1): 138-144.

Herrero, A. and E. Flores. 2008. *The cyanobacteria: Molecular biology, genomics and evolution*. Caister Academic Press.

Hildebrand, H., K. Mackenzie and F. Kopinke. 2009. Highly active Pd-on-magnetite nanocatalysts for aqueous phase hydrodechlorination reactions. *Environmental Science and Technology* 43(9): 3254-3259.

Ho, Y. P. and K. W. Leong. 2010. Quantum dot-based theranostics. *Nanoscale* 2(1): 60-68.

Ispas, C., D. Andreescu, A. Patel, D. V. Goia, S. Andreescu and K. N. Wallace. 2009. Toxicity and developmental defects of different sizes and shape nickel nanoparticles in zebrafish. *Environmental Science and Technology* 43(16): 6349-6356.

Jaiswal, J. K. and S. M. Simon. 2007. Optical monitoring of single cells using quantum dots. *Methods in Molecular Biology* 37493-104.

King-Heiden, T. C., P. N. Wiecinski, A. N. Mangham, K. M. Metz, D. Nesbit, J. A. Pedersen, R. J. Hamers, W. Heideman and R. E. Peterson. 2009. Quantum dot nanotoxicity assessment using the zebrafish embryo. *Environmental Science and Technology* 43(5): 1605-1611.

Lam, C., J. T. James, R. McCluskey and R. L. Hunter. 2004. Pulmonary toxicity of single-wall carbon nanotubes in mice 7 and 90 days after intractracheal instillation. *Toxicological Sciences* 77(1): 126-134.

Lewinski, N. A., H. Zhu, H. E. Jo, D. Pham, R. R. Kamath, C. R. Ouyang, C. D. Vulpe, V. L. Colvin and R. A. Drezek. 2010. Quantification of water solubilized CdSe/ZnS quantum dots in Daphnia magna. *Environmental Science and Technology* 44(5): 1841-1846.

Lu, C. M., C. W. Chau and J. H. Zhang. 2000. Acute toxicity of excess mercury on the photosynthetic performance of cyanobacterium, S. platensis - Assessment by chlorophyll fluorescence analysis. *Chemosphere* 41(1-2): 191-196.

Magrez, A., S. Kasas, V. Salicio, N. Pasquier, J. W. Seo, M. Celio, S. Catsicas, B. Schwaller and L. Forró. 2006. Cellular toxicity of carbon-based nanomaterials. *Nano Letters* 6(6): 1121-1125.

Mahendra, S., H. Zhu, V. L. Colvin and P. J. Alvarez. 2008. Quantum dot weathering results in microbial toxicity. *Environmental Science and Technology* 42(24): 9424-9430.

Marin, K., M. Stirnberg, M. Eisenhut, R. Krämer and M. Hagemann. 2006. Osmotic stress in Synechocystis sp. PCC 6803: Low tolerance towards nonionic osmotic stress results from lacking activation of glucosylglycerol accumulation. *Microbiology* 152(7): 2023-2030.

Michalet, X., F. F. Pinaud, L. A. Bentolila, J. M. Tsay, S. Doose, J. J. Li, G. Sundaresan, A. M. Wu, S. S. Gambhir and S. Weiss. 2005. Quantum dots for live cells, in vivo imaging, and diagnostics. *Science* 307(5709): 538-544.

Miller, L.A. 1982. *Practical rapid embedding procedure for transmission electron microscopy*. Laboratory Medicine 13:752-756.

Mitsui, A., S. Kumazawa and A. Takahashi. 1986. Strategy by which nitrogen-fixing unicellular cyanobacteria grow photoautotrophically. *Nature* 323(6090): 720-722.

Monteiro, D. R., L. F. Gorup, A. S. Takamiya, A. C. Ruvollo-Filho, E. R. d. Camargo and D. B. Barbosa. 2009. The growing importance of materials that prevent microbial adhesion: antimicrobial effect of medical devices containing silver. *International journal of antimicrobial agents* 34(2): 103-110.

Mueller, N. C. and B. Nowack. 2008. Exposure modeling of engineered nanoparticles in the environment. *Environmental Science and Technology* 42(12): 4447-4453.

Navarro, E., F. Piccapietra, B. Wagner, F. Marconi, R. Kaegi, N. Odzak, L. Sigg and R. Behra. 2008. Toxicity of silver nanoparticles to Chlamydomonas reinhardtii. *Environmental Science and Technology* 42(23): 8959-8964.

Nel, A., T. Xia, L. Mädler and N. Li. 2006. Toxic potential of materials at the nanolevel. S*cience* 311(5761): 622-627.

Nishikawa, K., Y. Yamakoshi, I. Uemura and N. Tominaga. 2003. Ultrastructural changes in Chlamydomonas acidophila (Chlorophyta) induced by heavy metals and polyphosphate metabolism. *FEMS microbiology ecology* 44(2): 253-259.

Nutt, M. O., K. N. Heck, P. Alvarez and M. S. Wong. 2006. Improved Pd-on-Au bimetallic nanoparticle catalysts for aqueous-phase trichloroethene hydrodechlorination. *Applied Catalysis B: Environmental* 69(1-2): 115-125.

Oberdörster, G., E. Oberdörster and J. Oberdörster. 2005. Nanotoxicology: An emerging discipline evolving from studies of ultrafine particles. *Environmental health perspectives* 113(7): 823-839.

Okamoto, N. and I. Inouye. 2005. Evolution: A secondary symbiosis in progress? *Science* 310(5746): 287.

Olafson, R. W., K. Abel and R. G. Sim. 1979. Prokaryotic metallothionein: Preliminary characterization of a blue-green alga heavy metal-binding protein. *Biochemical and biophysical research communications* 89(1): 36-43.

Ozturk, S. and B. Aslim. 2010. Modification of exopolysaccharide composition and production by three cyanobacterial isolates under salt stress. *Environmental Science and Pollution Research* 17(3): 595-602.

Pandhal, J., S. Y. Ow, P. C. Wright and C. A. Biggs. 2009. Comparative proteomics study of salt tolerance between a nonsequenced extremely halotolerant cyanobacterium and its mildly halotolerant relative using in vivo metabolic labeling and in vitro isobaric labeling. *Journal of Proteome Research* 8(2): 818-828.

Powers, K. W., S. C. Brown, V. B. Krishna, S. C. Wasdo, B. M. Moudgil and S. M. Roberts. 2006. Research strategies for safety evaluation of nanomaterials. Part VI. characterization of nanoscale particles for toxicological evaluation. *Toxicological Sciences* 90(2): 296-303.

Prasad, S. M., J. B. Singh, L. C. Rai and H. D. Kumar. 1991. Metal-induced inhibition of photosynthetic electron transport chain of the cyanobacterium Nostoc muscorum. *FEMS microbiology letters* 82(1): 95-100.

Press, D., T. D. Ladd, B. Zhang and Y. Yamamoto. 2008. Complete quantum control of a single quantum dot spin using ultrafast optical pulses. *Nature* 456(7219): 218-221.

Rachlin, J. W., T. E. Jensen and B. E. Warkentine. 1985. Morphometric analysis of the response of Anabaena flos-aquae and Anabaena variabilis (Cyanophyceae) to selected concentrations of zinc. *Archives of Environmental Contamination and Toxicology* 14(4): 395-402.

Rachlin, J. W., T. E. Jensen and B. Warkentine. 1984. The toxicological response of the alga Anabaena flos-aquae (Cyanophyceae) to cadmium. *Archives of Environmental Contamination and Toxicology* 13(2): 143-151.

Rangsayatorn, N., E. S. Upatham, M. Kruatrachue, P. Pokethitiyook and G. R. Lanza. 2002. Phytoremediation potential of Spirulina (Arthrospira) platensis: Biosorption and toxicity studies of cadmium. *Environmental Pollution* 119(1): 45-53.

Renault, S., M. Baudrimont, N. Mermer-Dudons, P. Gonzalez, S. Mornet and A. Brisson. 2008. Impacts of gold nanoparticle exposure on two freshwater species: A phytoplanktonic alga (Scenedesmus subspicatus) and a benthic bivalve (Corbicula fluminea). *Gold Bulletin* 41(2): 116-126.

Saker, M., C. Moreira, J. Martins, B. Neilan and V. M. Vasconcelos. 2009. DNA profiling of complex bacterial populations: Toxic cyanobacterial blooms. *Applied Microbiology and Biotechnology* 85(2): 237-252.

Sas, K. N., L. Kovács, O. Zsíros, Z. Gombos, G. Garab, L. Hemmingsen and E. Danielsen. 2006. Fast cadmium inhibition of photosynthesis in cyanobacteria in vivo and in vitro studies using perturbed angular correlation of γ-rays. *Journal of Biological Inorganic Chemistry* 11(6): 725-734.

Seufferheld, M. J., H. M. Alvarez and M. E. Farias. 2008. Role of polyphosphates in microbial adaptation to extreme environments. *Applied and Environmental Microbiology* 74(19): 5867-5874.

Su, C. K., C. W. Huang, C. S. Yang, Y. J. Wang and Y. C. Sun. 2010. In vivo monitoring of quantum dots in the extracellular space using push-pull perfusion sampling, online in-tube solid phase extraction, and inductively coupled plasma mass spectrometry. *Analytical Chemistry* 82(17): 7096-7102.

Sudhir, P., D. Pogoryelov, L. Kovács, G. Garab and S. D. S. Murthy. 2005. The effects of salt stress on photosynthetic electron transport and thylakoid membrane proteins in the cyanobacterium Spirulina platensis. *Journal of Biochemistry and Molecular Biology* 38(4): 481-485.

Sukhanova, A., J. Devy, L. Venteo, H. Kaplan, M. Artemyev, V. Oleinikov, D. Klinov, M. Pluot, J. H. M. Cohen and I. Nabiev. 2004. Biocompatible fluorescent nanocrystals for immunolabeling of membrane proteins and cells. *Analytical Biochemistry* 324(1): 60-67.

Surosz, W. and K. A. Palinska. 2004. Effects of heavy-metal stress on cyanobacterium Anabaena flos-aquae. *Archives of Environmental Contamination and Toxicology* 48(1): 40-48.

Tamoi, M., H. Kurotaki and T. Fukamizo. 2007. β-1,4-Glucanase-like protein from the cyanobacterium Synechocystis PCC6803 is a β-1,3-1,4-glucanase and functions in salt stress tolerance. *Biochemical Journal* 405(1): 137-146.

Turner, J. S. and N. J. Robinson. 1995. Cyanobacterial metallothioneins: Biochemistry and molecular genetics. *Journal of industrial microbiology* 14(2): 119-125.

Vallarta Jr., R., Cao, E., and Y.R. Sibal. 1998. *Cadmium Uptake in Synechococcus aquatilis (Reynaud) Strain SY01*. *ScienceDiliman* **10**.

Van Hoecke, K., K. A. C. De Schamphelaere, P. Van Der Meeren, G. Smagghe and C. R. Janssen. 2011. Aggregation and ecotoxicity of CeO2 nanoparticles in synthetic and natural waters with variable pH, organic matter concentration and ionic strength. *Environmental Pollution* 159(4): 970-976.

Verma, A. and F. Stellacci. 2010. Effect of surface properties on nanoparticle-cell interactions. *Small* 6(1): 12-21.

Vymazal, J. 1987. Toxicity and accumulation of cadmium with respect to algae and cyanobacteria: a review. *Toxicity Assessment* 2(4): 387-415.

Wokovich, A., K. Tyner, W. Doub, N. Sadrieh and L. F. Buhse. 2009. Particle size determination of sunscreens formulated with various forms of titanium dioxide. *Drug development and industrial pharmacy* 35(10): 1180-1189.

Xia, L., S. C. Lenaghan, M. Zhang, Z. Zhang and Q. Li. 2010. Naturally occurring nanoparticles from English ivy: An alternative to metal-based nanoparticles for UV protection. *Journal of Nanobiotechnology* 8.

Xing, Y. and J. Rao. 2008. Quantum dot bioconjugates for in vitro diagnostics & in vivo imaging. *Cancer Biomarkers* 4(6): 307-319.

Xing, Y., Z. Xia and J. Rao. 2009. Semiconductor quantum dots for biosensing and in vivo imaging. *IEEE Transactions on Nanobioscience* 8(1): 4-12.

Yang, H. 2010. Nanoparticle-mediated brain-specific drug delivery, imaging, and diagnosis. *Pharmaceutical research* 27(9): 1759-1771.

Yee, N., L. G. Benning, V. R. Phoenix and F. G. Ferris. 2004. Characterization of Metal-Cyanobacteria Sorption Reactions: A Combined Macroscopic and Infrared Spectroscopic Investigation. *Environmental Science and Technology* 38(3): 775-782.

Zeng, J. and W. Wang. 2009. The importance of cellular phosphorus in controlling the uptake and toxicity of cadmium and zinc in Microcystis aeruginosa, a freshwater cyanobacterium. *Environmental Toxicology and Chemistry* 28(8): 1618-1626.

Zeng, J., L. Yang and W. Wang. 2009. Acclimation to and recovery from cadmium and zinc exposure by a freshwater cyanobacterium, Microcystis aeruginosa. *Aquatic Toxicology* 93(1): 1-10.

Zhang, B., Y. Luo and Q. Wang. 2010. Development of silver-zein composites as a promising antimicrobial agent. *Biomacromolecules* 11(9): 2366-2375.

Zhang, L. W. and N. A. Monteiro-Riviere. 2009. Mechanisms of quantum dot nanoparticle cellular uptake. *Toxicological Sciences* 110(1): 138-155.

Zhang, X., H. Sun and Z. Zhang. 2006. Bioaccumulation of titanium dioxide nanoparticles in carp. *Huanjing Kexue/Environmental Science* 27(8): 1631-1635.